Research Article

The osmotic stress–activated receptor-like kinase DPY1 mediates SnRK2 kinase activation and drought tolerance in *Setaria*

Meicheng Zhao [1,*,†] Qi Zhang [1,†] Hong Liu [1,2,†] Sha Tang [3] Chunyue Shang [1,4] Wei Zhang [3] Yi Sui [3] Yuxue Zhang [1] Chunyan Zheng [1] Hui Zhang [3] Cuimei Liu [5] Jinfang Chu [5,6] Guanqing Jia [3] Haigang Wang [4] Xigang Liu [2,7] Diaoguo An [1] Feng Zhu [1] Hui Zhi [3] Chuanyin Wu [3] and Xianmin Diao [3,7,*]

1 Key Laboratory of Agricultural Water Resources, Hebei Key Laboratory of Soil Ecology, Center for Agricultural Resources Research, Institute of Genetics and Developmental Biology, Chinese Academy of Sciences, Shijiazhuang 050021, China

2 Ministry of Education Key Laboratory of Molecular and Cellular Biology, Hebei Key Laboratory of Molecular and Cellular Biology, College of Life Sciences, Hebei Normal University, Shijiazhuang 050024, China

3 Institute of Crop Sciences, Chinese Academy of Agricultural Sciences, Beijing 100081, China

4 Center for Agricultural Genetic Resources Research, Shanxi Agricultural University, Taiyuan 030031, China

5 National Centre for Plant Gene Research (Beijing), Institute of Genetics and Developmental Biology, Chinese Academy of Sciences, Beijing 100101, China

6 College of Advanced Agricultural Sciences, University of Chinese Academy of Sciences, Beijing 100049, China

7 Hebei Collaboration Innovation Center for Cell Signaling, Hebei Normal University, Shijiazhuang 050024, China

*Author for correspondence: mczhao@sjziam.ac.cn (M.Z.), diaoxianmin@caas.cn (X.D.)

†These authors contributed equally.

The author responsible for distribution of materials integral to the findings presented in this article in accordance with the policy described in the Instructions for Authors (https://academic.oup.com/plcell/pages/General-Instructions) are: Meicheng Zhao (mczhao@sjziam.ac.cn), Xianmin Diao (diaoxianmin@caas.cn).

Abstract

Plant genomes encode many receptor-like kinases (RLKs) that localize to the cell surface and perceive a wide variety of environmental cues to initiate downstream signaling cascades. Whether these RLKs participate in dehydration stress signaling in plants is largely unknown. DROOPY LEAF1 (DPY1), a leucine-rich repeat (LRR)-RLK, was recently shown to regulate plant architecture by orchestrating early brassinosteroid signaling in foxtail millet (*Setaria italica*). Here, we show that DPY1 is essential for the acclimation of foxtail millet to drought stress. DPY1 can be phosphorylated and activated in response to osmotic stress and is required for more than half of osmotic stress–induced global phosphorylation events, including the phosphorylation of sucrose nonfermenting kinase 2s (SnRK2s), the central kinases involved in osmotic stress. DPY1 acts upstream of STRESS-ACTIVATED PROTEIN KINASE 6 (SAPK6, a subclass I SnRK2) and is required for full SAPK6 activation, thereby allowing regulation of downstream genes to mount a response against drought stress. These signaling events are largely independent of DPY1-mediated brassinosteroid signaling. The DPY1-SAPK6 module is specific to seed plants and is absent in ancestral nonseed plants. Our findings reveal a dehydration stress–activated RLK that plays an indispensable role in osmotic stress signaling and mediates SnRK2 activation at the cell surface.

Introduction

Drought is a major abiotic stress that seriously limits plant growth and threatens crop yields, potentially harming global food security (Gupta et al. 2020). Breeding drought-tolerant crops via genetic improvement is a useful way to cope with this challenge. Indigenous crops, especially those grown in

IN A NUTSHELL

Background: To protect themselves from drought-induced damage, plants must sense the osmotic stress that accompanies drought and rapidly transmit a signal, triggering defense responses to acclimate to water deficit. When plants sense dehydration stress, SNF1-RELATED PROTEIN KINASE2 (SnRK2) family members are activated, representing a key event in dehydration signaling. Although this step was elucidated ~20 years ago, the upstream components that activate SnRK2 kinases remain unknown. We previously identified the transmembrane kinase DROOPY LEAF1 (DPY1) as a key regulator of plant architecture in foxtail millet (*Setaria italica*). A screen for DPY1-interacting proteins identified a member of the SnRK2 family, suggesting that DPY1 might be involved in SnRK2-mediated dehydration signaling.

Question: Is DPY1 an upstream component required for SnRK2 activation in response to dehydration stress? As a plasma membrane–anchored receptor-like kinase, how does DPY1 respond to dehydration stress?

Findings: DPY1 is crucial for plant acclimation to drought stress. Loss of DPY1 function enhanced susceptibility to drought, partially due to impaired osmotic signaling. DPY1 is phosphorylated and activated in response to osmotic stress and is required for over 50% of osmotic stress–triggered global phosphorylation events, including that of SnRK2s, the central kinases in osmotic stress. DPY1 interacts with but cannot directly phosphorylate STRESS-ACTIVATED PROTEIN KINASE6 (SAPK6), a subclass I SnRK2, but it is required for full SAPK6 activation and the regulation of downstream genes. This activation is largely independent of DPY1-mediated brassinosteroid signaling. Therefore, DPY1 is a key missing component in osmotic stress signaling that mediates SnRK2 activation when plants encounter drought stress.

Next steps: Despite the discovery of DPY1-based osmotic stress signaling, numerous gaps remain to be addressed. We plan to focus on identifying the mechanism of DPY1 activation by osmotic stress and components linking DPY1 and SnRK2s.

arid and semiarid regions, hold great promise. For example, foxtail millet (*Setaria italica*) is an ideal model system from which to learn mechanisms of plant responses to dehydration stress due to its extremely high drought tolerance. Indeed, seed germination of foxtail millet is successful using water at only 26% of seed weight, in contrast to at least 45% in other cereals (Diao et al. 2014).

Plants sense dehydration stress and transduce the stimulus to elicit acclimation responses, such as global changes in gene expression and various physiological parameters (Zhu 2016; Gupta et al. 2020). In Arabidopsis (*Arabidopsis thaliana*), a group of sucrose nonfermenting 1 (SNF1)–related protein kinase 2s (SnRK2s) has been identified as central signal transmitters of dehydration stress (Zhu 2016; Lin et al. 2020; Soma et al. 2020). SnRK2s are classified into 3 subclasses in angiosperm plants according to sequence similarity (Kobayashi et al. 2004). Subclass III SnRK2s (SnRK2.2, SnRK2.3, and SnRK2.6), an ancestral form of SnRK2s in evolution (Saruhashi et al. 2015), are strongly activated by both osmotic stress and the phytohormone abscisic acid (ABA), and they are well known as central players in ABA signaling (Mustilli et al. 2002; Boudsocq et al. 2004; Umezawa et al. 2009). In addition, seed plants have evolved other types of SnRK2s, specifically subclass I SnRK2s (Arabidopsis SnRK2.1, SnRK2.4, SnRK2.5, and SnRK2.10; rice [*Oryza sativa*] STRESS-ACTIVATED PROTEIN KINASE 4–7 [SAPK4–7]), which are activated by osmotic stress in an ABA-independent manner (Boudsocq et al. 2004; Kobayashi et al. 2004). The development of subclass I SnRK2s is thus regarded as an adaptive evolutionary mechanism of

seed plants to cope with a constantly changing terrestrial environment (Soma et al. 2017, 2020; Shinozawa et al. 2019).

Although the activation of SnRK2s induced by osmotic stress was first described 20 years ago (Boudsocq et al. 2004; Kobayashi et al. 2004), the underlying activation mechanisms have only recently been elucidated. Saruhashi et al (2015) reported that, in the moss *Physcomitrium patens*, the ancestral group B Raf-like kinase (RAF) ABA and abiotic stress–responsive Raf-like kinase (ARK) acts as an upstream kinase to directly phosphorylate and activate ABA- and osmotic stress–responsive PpSnRK2s (Saruhashi et al. 2015). Recently, 4 independent studies almost simultaneously demonstrated that the activation of Arabidopsis SnRK2s in response to osmotic stress also requires phosphorylation by upstream B group RAF kinases (Fàbregas et al. 2020; Katsuta et al. 2020; Lin et al. 2020; Soma et al. 2020; Takahashi et al. 2020). Thus, RAF-SnRK2 signaling cascades represent an evolutionarily conserved module that emerged in bryophytes such as *P. patens* and in Arabidopsis.

These SnRK2-interacting RAF proteins lack transmembrane and extracellular domains and localize to the cytoplasm (Lin et al. 2020), making them likely to act as intermediate signal transmitters of osmotic stress to activate SnRK2s. Importantly, the putative cell surface components responsible for SnRK2 activation in plants remain unknown. In yeast (*Saccharomyces cerevisiae*), a membrane-anchored histidine kinase (HK) was proposed to act as an osmotic stress sensor, with signal transduction initiated by activation via autophosphorylation at a specific His residue after sensing

osmotic changes. The signal is then transmitted to a downstream mitogen-activated protein kinase (MAPK) cascade, resulting in protective responses (Maeda et al. 1994; Hohmann 2002). A recent study in *P. patens* showed that the activation of PpSnRK2s and RAF phosphorylation evoked by ABA and osmotic stress depend on a group of endoplasmic reticulum (ER)–anchored ethylene receptor–related HKs, suggesting that HKs act as upstream components required for RAF and SnRK2 activation (Toriyama et al. 2022).

The plasma membrane is a signaling interface used by plants to sense environmental changes, from which signals are transmitted to downstream targets (Verslues et al. 2022), although the underlying details remain poorly understood. Receptor-like kinases (RLKs) form one of the largest protein families in plants and usually function at the cell surface as sensors/receptors of varied small molecules or ligands to initiate signaling cascades (Osakabe et al. 2013). Among the more than 600 RLKs in Arabidopsis, only a few have been linked to the regulation of specific responses to abiotic stress (Osakabe et al. 2013), such as RECEPTOR-LIKE PROTEIN KINASE1 (RPK1), BRI1-ASSOCIATED KINASE1 (BAK1), and GUARD CELL HYDROGEN PEROXIDE-RESISTANT1 (GHR1), which all contribute to early ABA signaling to regulate stomatal closure and other responses (Osakabe et al. 2005; Hua et al. 2012; Shang et al. 2016; Deng et al. 2022). So far, it is still largely unknown whether and how plant RLKs function in dehydration stress.

We recently revealed that DROOPY LEAF1 (DPY1), a member of the leucine-rich repeat (LRR)-RLK II subfamily, modulates plant architecture by blocking early brassinosteroid (BR) signaling in foxtail millet (Zhao et al. 2020; Wang et al. 2021). DPY1 homologs in Arabidopsis form a group of kinases called NSP-INTERACTING KINASEs (NIKs) and CLAVATA3 INSENSITIVE RECEPTOR KINASEs (CIKs), which play essential roles in multiple signaling pathways, including antiviral and antibacterial immunity as well as the regulation of stem cell fate mediated by the small peptide CLV3 (Carvalho et al. 2008; Hu et al. 2018; Li et al. 2019).

Here, we show that DPY1 is required for osmotic signal transduction and is essential for plant acclimation to drought. A quantitative phosphoproteomic analysis revealed that DPY1 is responsible, directly or indirectly, for at least half of all osmotic stress–induced phosphorylation sites. Among these, we identified SAPK6 as a key downstream target of DPY1 for osmotic signaling, whose full activation and regulation of downstream gene expression are DPY1 dependent. We also demonstrate that the DPY1-SAPK6 module only exists in angiosperm plants and is missing in ancestral nonseed plants. Our findings reveal an indispensable LRR-RLK in osmotic signaling and connect SnRK2 activation to a cell surface–localized RLK.

Results

DPY1 interacts with SAPK6, a subclass I SnRK2

We set out to identify potential DPY1-interacting proteins. To this end, we immunoprecipitated (IP) DPY1-FLAG from *Ubipro:*
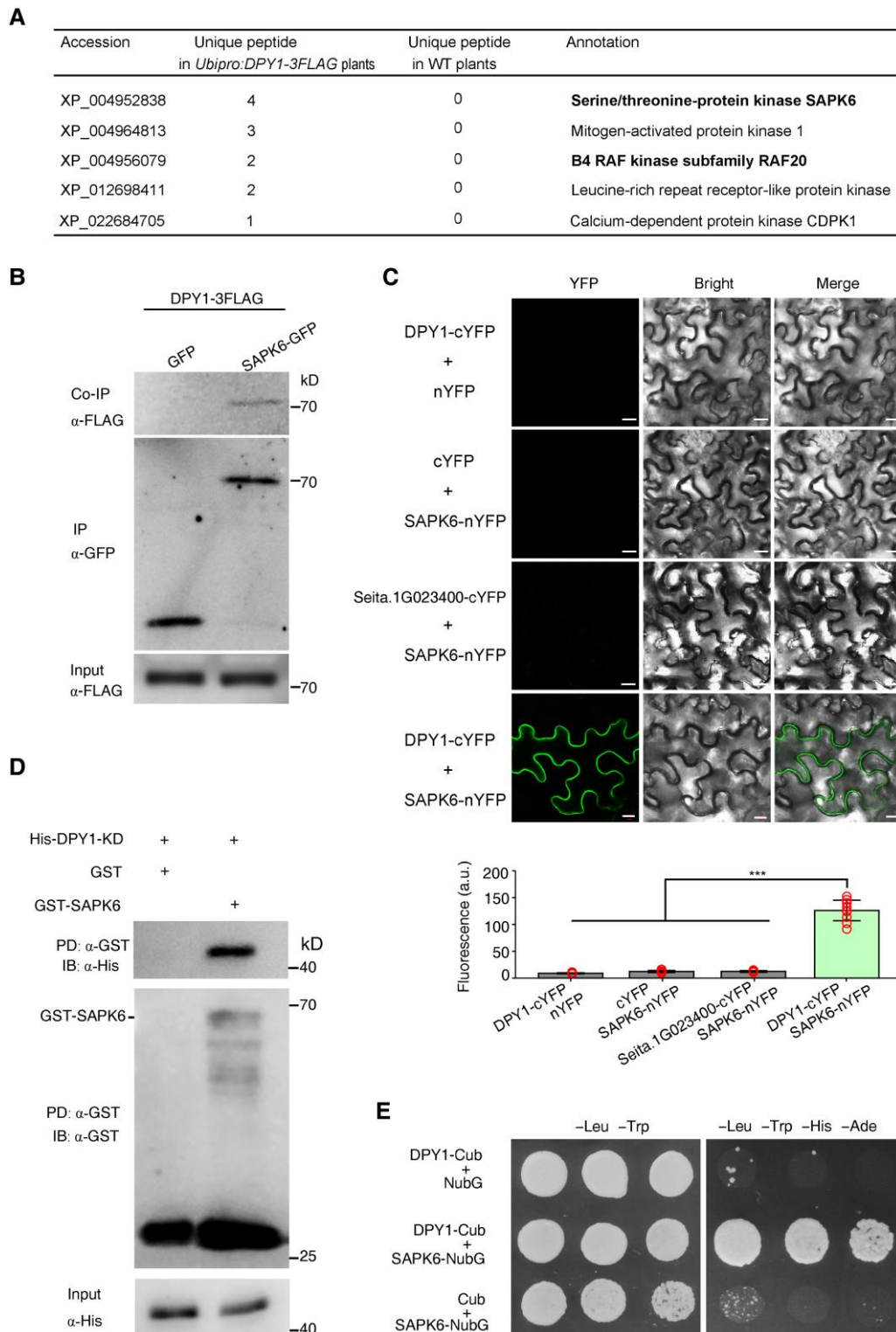
DPY1-3FLAG (DPY1-OE) transgenic plants and subjected the immunoprecipitates to liquid chromatography–tandem mass spectrometry (LC–MS/MS) analysis. We identified 5 protein kinases out of 377 high-confidence DPY1-interacting proteins (Fig. 1A; Supplemental Data Set S1). Among them, we noticed the subclass I SnRK2 protein kinase SAPK6 (XP_004952838.2) and the B4 subclass RAF20 (XP_004956079.1) (Supplemental Figs. S1 and S2). Their putative orthologs in Arabidopsis and *P. patens* were recently shown to form a kinase complex that transduces osmotic stress signals (Saruhashi et al. 2015; Lin et al. 2020; Soma et al. 2020), suggesting that DPY1 might be also involved in osmotic stress signaling in foxtail millet.

We determined the subcellular localization of SAPK6-green fluorescent protein (GFP) and DPY1-GFP in transiently transfected foxtail millet protoplasts and stable transgenic lines, respectively. We detected SAPK6-GFP mainly in the cytoplasm and nucleus of transfected protoplasts (Supplemental Fig. S3A), similar to its putative orthologs in Arabidopsis (SnRK2.1, also named SRK2G) and moss (PpSnRK2B) (Saruhashi et al. 2015; Soma et al. 2017). In contrast, DPY1-GFP specifically localized to the plasma membrane, as observed in foxtail millet protoplasts (Supplemental Fig. S3A) and leaf blades of a *dpy1* mutant complemented with the *DPY1pro:DPY-GFP* transgene (Supplemental Fig. S3B). Their subcellular localization did not obviously change following short PEG treatment for 30 min in protoplasts or natural drought stress in plants (Supplemental Fig. S3). To validate the interaction of DPY1 with SAPK6 in vivo, we performed a coimmunoprecipitation (Co-IP) assay with an anti-GFP antibody using foxtail millet leaf protoplasts prepared from *Ubipro:DPY1-3FLAG* plants that were transiently transfected with a *35Spro:SAPK6-GFP* or *35Spro:GFP* construct. We established that DPY1-3FLAG can be IP with SAPK6-GFP, but not GFP (Fig. 1B), demonstrating the association of DPY1 and SAPK6 in plants.

We confirmed this association by a bimolecular fluorescence complementation (BiFC) assay in *Nicotiana benthamiana* leaves (Fig. 1C), as evidenced by the green fluorescence detected near the plasma membrane in cells coexpressing DPY1-cYFP and SAPK6-nYFP, but not when DPY1-cYFP was coexpressed with Seita.1G023400, encoding an LRR-RLK II family member and close relative of DPY1 (Fig. 1C). Furthermore, a glutathione S-transferase (GST) pull-down (PD) assay showed that recombinant His-tagged DPY1 physically interacts with GST-SAPK6 (Fig. 1D). Finally, as DPY1 localized to the plasma membrane, we performed a split-ubiquitin–based yeast 2-hybrid assay, which validated the direct interaction of DPY1 and SAPK6 in vitro (Fig. 1E). These findings indicate that SAPK6 is a true DPY1-interacting protein in foxtail millet.

DPY1 evolved in seed plants but not in ancestral nonseed plants

Previous phylogenic analyses of the SnRK2 family across plants demonstrated that subclass I-type SnRK2s have

A

Accession	Unique peptide in *Ubipro:DPY1-3FLAG* plants	Unique peptide in WT plants	Annotation
XP_004952838	4	0	**Serine/threonine-protein kinase SAPK6**
XP_004964813	3	0	Mitogen-activated protein kinase 1
XP_004956079	2	0	**B4 RAF kinase subfamily RAF20**
XP_012698411	2	0	Leucine-rich repeat receptor-like protein kinase
XP_022684705	1	0	Calcium-dependent protein kinase CDPK1

B

C

D

E

Figure 1. DPY1 directly interacts with SAPK6. **A)** Potential DPY1-interacting kinases identified by Co-IP–MS/MS from transgenic plants harboring *Ubipro:DPY1-3FLAG*. WT plants were used as a background control. SAPK6, a member of subclass I SnRK2s, and its upstream activating kinase, RAF20, are highlighted in bold. **B)** Co-IP assay showing that DPY1 interacts with SAPK6 in vivo. Protein extracts from protoplasts of transgenic *Ubipro:DPY1-3FLAG* plants transiently expressing SAPK6-GFP or GFP were IP with GFP-Trap magnetic beads and IB with an anti-FLAG antibody. The experiments were performed twice with similar results. **C)** BiFC assays validating the interaction between DPY1 and SAPK6 in *N. benthamiana* epidermal cells. Seita.1G023400, encoding a protein closely related to DPY1 in the LRR-RLK II family (see Fig. 2), was used a negative control. Proteins were fused to either the C-terminal or the N-terminal half of the yellow fluorescent protein (cYFP/nYFP). Scale bars, 10 μm. Quantitative measurements of the interaction are performed based on the mean fluorescence intensity of images ($n = 10$). The values are means $\pm$ SD. ***$P < 0.001$

(continued)
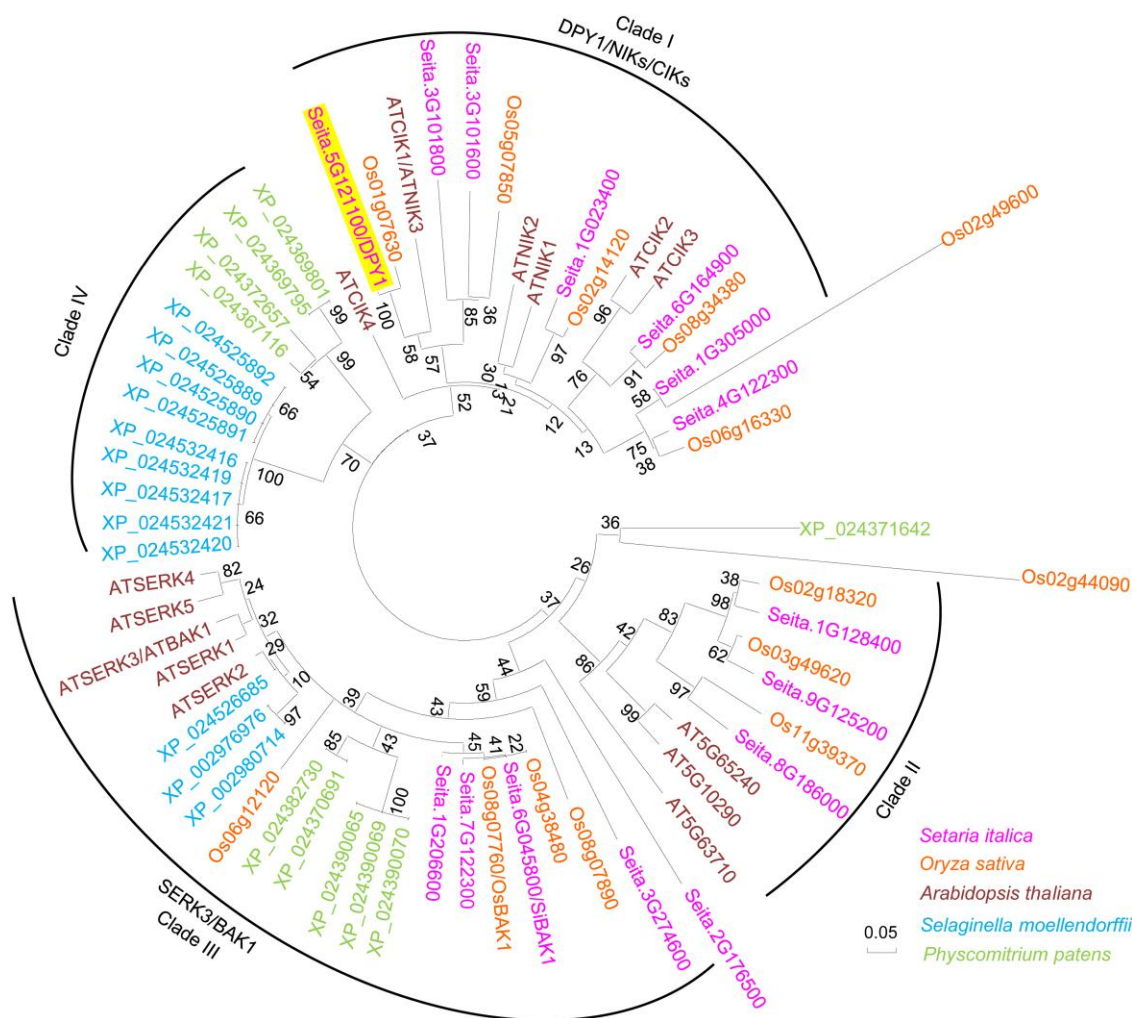
Figure 2. DPY1-related members exist in seed plants but not in ancestral nonseed plants. A neighbor-joining tree was constructed based on the LRR-RLK II members from Arabidopsis and their corresponding homologs in rice (*O. sativa*), foxtail millet (*S. italica*), and the ancestral nonseed plants *S. moellendorffii* and *P. patens*. The full-length amino acid sequences were aligned using Mega5 software with ClustalW to construct an un-rooted phylogenetic tree after bootstrap analysis for 1,000 replicates. The scale bar represents 0.05 nucleic acid substitutions per nucleotide position. The warm color for angiosperm plants (foxtail millet, rice, and Arabidopsis) and cool color for nonseed plants (*S. moellendorffii* and *P. patens*). DPY1 was highlighted in the phylogenetic tree.

evolved only in seed plants and are absent from the genomes of other nonseed plants (Sakata et al. 2014; Saruhashi et al. 2015; Soma et al. 2020). To investigate the evolutionary origin of DPY1, we obtained 12 and 10 putative homologous members showing at least 50% amino acid sequence identity with DPY1 from the genome databases of the lycophyte *Selaginella moellendorffii* and the moss *P. patens*, respectively. We then constructed a phylogenetic tree based on LRR-RLK

subfamily II members from Arabidopsis, rice, foxtail millet, *S. moellendorffii*, and *P. patens*. Clustering analysis revealed the presence of DPY1-like proteins only in seed plants, but not in the lycophyte or moss (Fig. 2). In contrast, the sister clade that included BAK1 (also named SOMATIC EMBRYOGENESIS RECEPTOR-LIKE KINASE [SERK3]) and SERK-like proteins, which function as coreceptors of multiple RLK-mediated signaling pathways (Li et al. 2002; Nam and Li

Figure 1. (Continued)

(Student's *t*-test). Red open circles represent sample data points. **D)** Validation of the DPY1/SAPK6 interaction by a GST PD assay. Recombinant GST-SAPK6 or GST was incubated with His-DPY1-KD, pulled down with GST beads, and IB with an anti-His antibody. The experiments were repeated 3 times independently with similar results. **E)** Yeast split-ubiquitin–based 2-hybrid assay showing the interaction of DPY1 with SAPK6. Positive colonies were spotted onto synthetic defined (SD) medium lacking Leu and Trp (−Leu −Trp) and SD medium lacking Leu, Trp, His, and Ade (−Leu, −Trp, −His, −Ade) at 3 dilutions (10-fold).
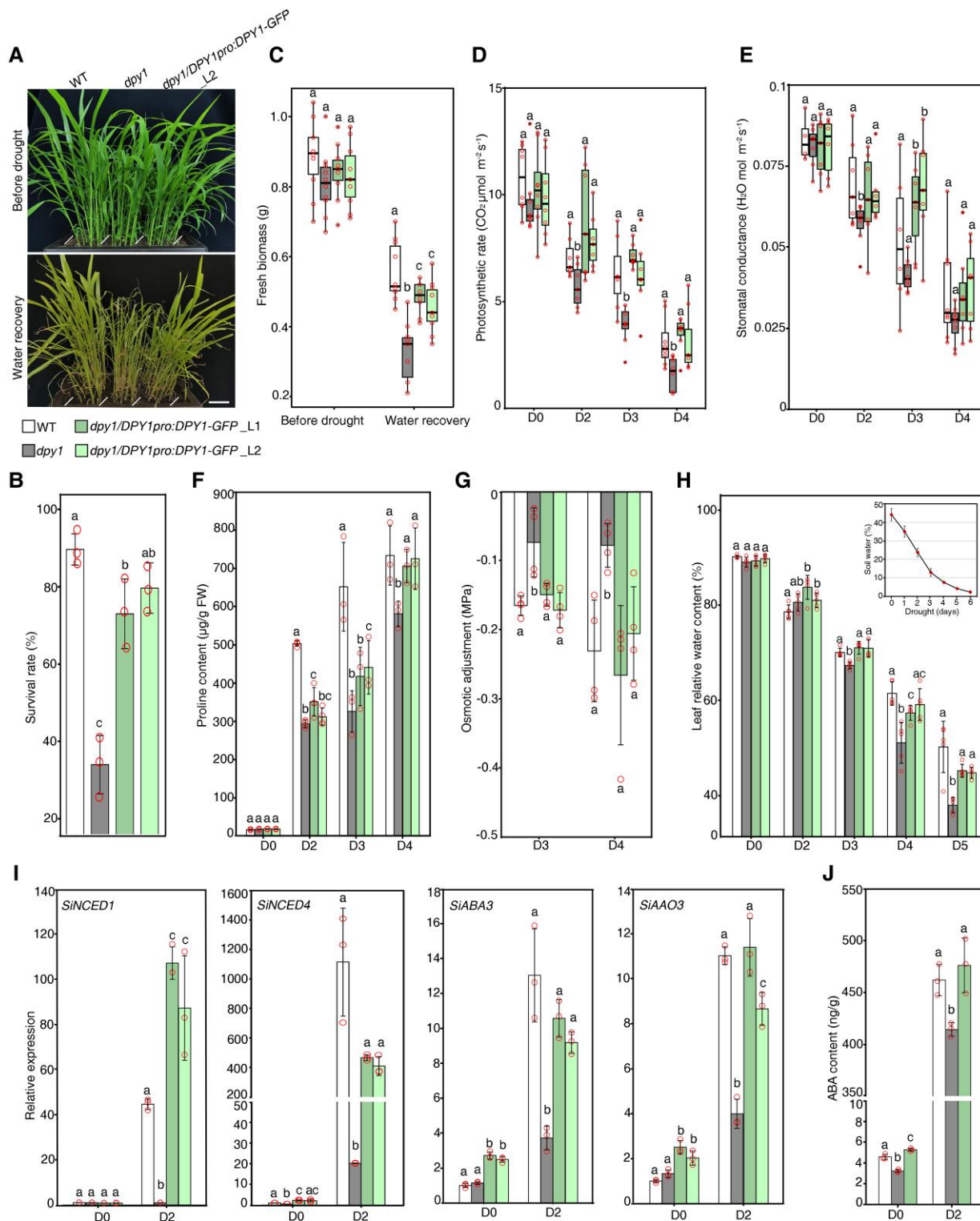
Figure 3. *Dpy1* plants are susceptible to drought. **A)** Drought tolerance phenotypes of WT (Yugu1), *dpy1*, and *dpy1/DPY1pro:DPY1-GFP* plants. Scale bar, 5 cm. All plants were grown under normal watering conditions for 18 d before being subjected to 6 d of drought treatment, followed by water recovery for 6 d (Supplemental Fig. S5). **B)** Survival rate of each genotype after 6 d of recovery. The values are means ± SD from 3 independent biological replicates ($n = 93$, total plants examined for each genotype). **C)** Fresh weight of shoots from each genotype before drought and after recovery via watering ($n = 10$). **D, E)** Photosynthetic efficiency **D)** and stomatal conductance **E)** during drought ($n = 7$). **C** to **E)** Boxplots show median (inner thick line) and interquartile range (box). The top and bottom of the box represent the 0.75 and 0.25 percentiles, respectively. The whiskers represent 1.5 times the interquartile range. All the sample points were shown with the open circles, and the circles out of the whiskers represent outliers. **F)** Proline accumulation in leaves during the drought time course. The values are means ± SD from 3 independent measurements (5 leaves per

(continued)

2002; Chinchilla et al. 2007), is widely conserved from the moss to seed plants (Fig. 2). This finding suggests that the DPY1 subclass, together with subclass I SnRK2s (Soma et al. 2020), was specifically acquired by seed plants.

DPY1 positively regulates plant drought tolerance

To evaluate whether *DPY1* functions in the osmotic stress response, we grew the wild type (WT, the inbred line Yugu1), the ethyl methanesulfonate (EMS) mutant *dpy1* (a loss-of-function mutant in the Yugu1 background, Supplemental Fig. S4) (Zhao et al. 2020), and *dpy1* complementation lines carrying a 7-kb *DPY1* genomic fragment cloned in-frame and upstream of *GFP* (*dpy1/DPY1pro: DPY1-GFP*) in the same pots for 18 d. We then subjected all plants to drought stress, which we administered by withholding water for 6 d (Supplemental Fig. S5A), during which the soil water content decreased from $40 \pm 2.3\%$ to $3.3 \pm 1.2\%$. We confirmed that each genotype experienced similar levels of drought by continuously monitoring soil water content and water potential (Supplemental Fig. S5B). We evaluated plant tolerance to drought by measuring their survival rates after rewatering. We observed that *dpy1* plants are less resistant than WT plants to drought stress, as shown by a survival rate of $35 \pm 8\%$ for *dpy1* and approximately $90 \pm 4\%$ for WT (Fig. 3, A and B; Supplemental Fig. S6). Accordingly, the fresh weight of *dpy1* plants decreased by $60 \pm 11\%$ after drought treatment compared to $37 \pm 9\%$ for WT plants (Fig. 3C). These defects were fully rescued in *dpy1/DPY1pro:DPY1-GFP* plants (Fig. 3, A to C). In addition, we monitored photosynthesis and transpiration parameters for each genotype during the drought period. Compared to WT and *dpy1/DPY1pro:DPY1-GFP* plants, *dpy1* plants exhibited a lower photosynthetic rate and lower stomatal conductance when exposed to drought (Fig. 3, D and E), supporting the notion that the *dpy1* mutant is more susceptible than the WT to drought.

To explore the physiological basis of the compromised drought tolerance in *dpy1* plants, we investigated the dynamics of the accumulation of the major osmoprotectant metabolite proline, osmotic adjustment (OA), as well as relative leaf water content (RLWC) during drought. We detected lower levels of proline in *dpy1* plants at each time point during the drought period compared to WT and *dpy1/DPY1pro: DPY1-GFP* plants (Fig. 3F). We also measured OA, which reflects the net accumulation of total solutes in a cell in response to stress, among the different genotypes. OA is calculated as the difference in osmotic potential at full turgor between the onset of drought (D0) and Day 3 into drought stress (D3) or D4 plants. In line with their lower proline content, *dpy1* plants displayed a smaller drop in OA compared to WT and *dpy1/DPY1pro:DPY1-GFP* plants after drought treatment (Fig. 3G). Finally, we investigated RLWC dynamics among the genotypes over the course of drought treatment. Although RLWC values were the same at D0 across all genotypes, they started to decline more rapidly in *dpy1* plants when the soil water content dropped to $\sim 13 \pm 1.5\%$ on Day 3 of drought. Indeed, RLWC in *dpy1* plants dropped by up to $57 \pm 2\%$ compared to WT ($44 \pm 6\%$) and *dpy1/ DPY1pro:DPY1-GFP* plants ($49 \pm 1\%$) by Day 5 of drought treatment (Fig. 3H). The greater water loss seen in *dpy1* plants might be caused by diminished osmoprotectant accumulation but not by changes in stomatal aperture. Taken together, these findings indicate that the defects in osmoprotectant accumulation and the maintenance of leaf water content caused by the loss of DPY1 function result in plant susceptibility to drought.

We also examined the induction of ABA biosynthesis genes in response to drought. Accordingly, we measured the expression levels of 4 putative ABA biosynthesis genes, *SiNCED1* (*NINE-CIS-EPOXYCAROTENOID DIOXYGENASE*), *SiNCED4*, *SiABA3* (*ABA DEFICIENT 3*), and *SiAAO3* (*ABSCISIC ALDEHYDE OXIDASE 3*), in plants at the D0 and D2, when the leaves were slightly dehydrated with leaf water content dropped by $9.7 \pm 1.7\%$ compared to D0. These genes were expressed at low levels at D0 but showed a massive induction ($\sim 1,000$-fold) following drought (Fig. 3I). Importantly, *dpy1* plants exhibited a much weaker induction in their expression compared to WT and *dpy1/DPY1pro: DPY1-GFP* plants. In addition, ABA contents were lower in *dpy1* plants, presumably due to the lower induction of ABA biosynthesis genes under drought conditions (Fig. 3J). These findings suggest that DPY1 is crucial for ABA biosynthesis and the early drought response.

We previously showed that BR signaling was hyperactivated in *dpy1* plants, resulting in the malformation of vascular sclerenchyma and low lignin content in leaves (Zhao et al. 2020), which might be linked to the greater drought susceptibility of *dpy1* plants. We therefore examined the role of elevated BR signaling in *dpy1* plants in the context of drought resistance. We applied the BR biosynthesis inhibitor

Figure 3. (Continued)
measurement). **G)** OA capability among the different genotypes during drought. OA was determined based on the difference in osmotic potential at full turgor between untreated (D0) and drought-treated (D3 or D4) plants. The values are means $\pm$ SD from 4 independent measurements (5 leaves per measurement). **H)** Relative water content of leaves (the second fully expanded leaf counted from the top) over the course of drought treatment ($n = 5$). **I)** RT-qPCR analysis of the expression levels of the foxtail millet ABA biosynthesis genes *SiNCED1*, *SiNCED4*, *SiABA3*, and *SiAAO3* at D0 and D2 among the indicated genotypes. The expression level in the D0 WT plants was set to 1.0. The values are means $\pm$ SD from 3 biological replicates. **J)** ABA contents in leaves (the second fully expanded leaf counted from the top) at D0 and D2 among the indicated genotypes. The values are means $\pm$ SD from 3 biological replicates. Different letters indicate significant differences ($P < 0.05$) within each growth condition or time point of drought, as determined by 1-way ANOVA with Tukey's multiple comparisons test. The open circles represent sample data points.
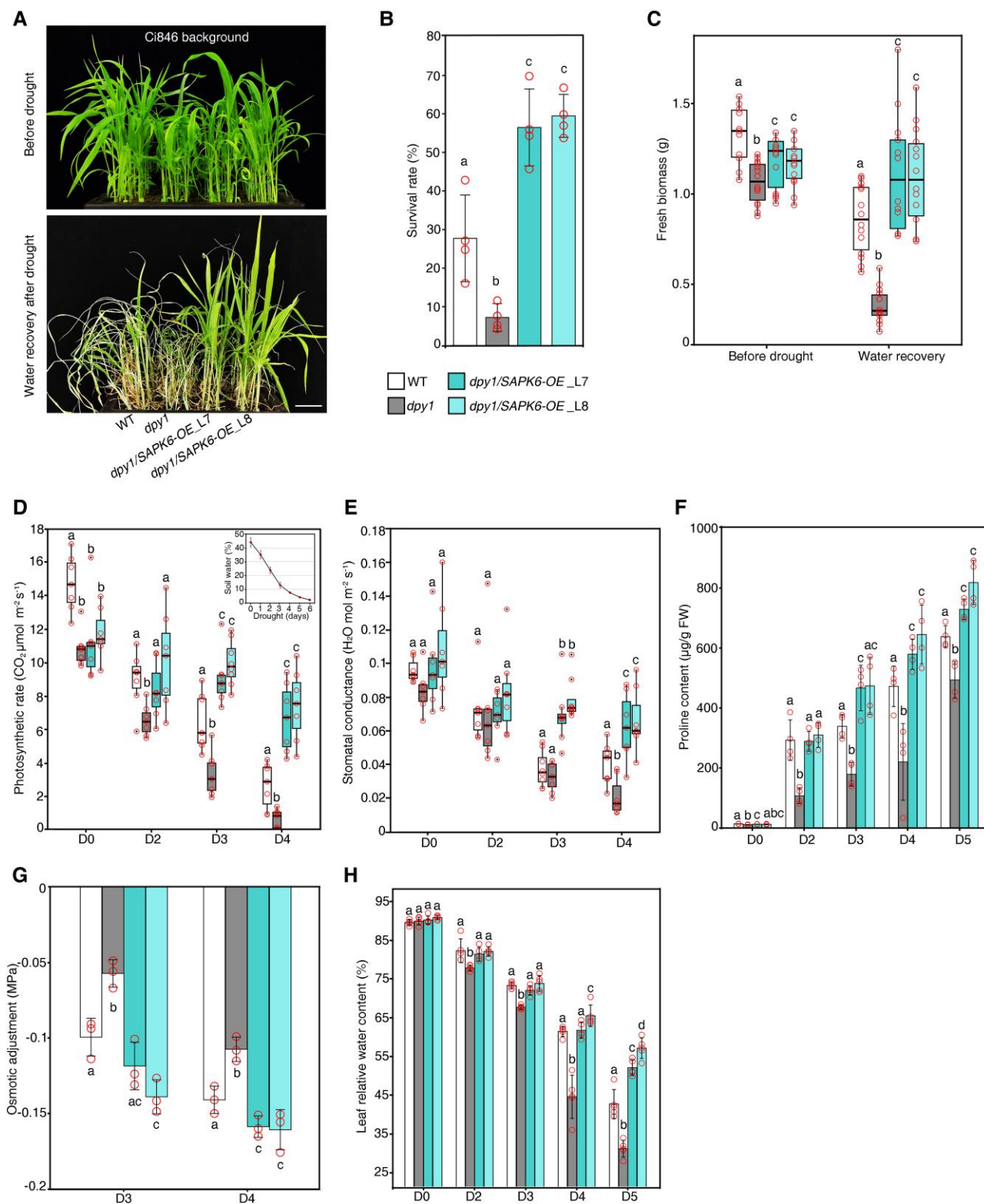
Figure 4. Overexpression of *SAPK6* rescues the drought susceptibility of *dpy1* plants. **A)** Drought tolerance phenotypes of WT (Ci846), *dpy1*, and *dpy1/Ubipro:SAPK6-3FLAG* (*dpy1/SAPK6-OE*) plants. Scale bar, 5 cm. All plants were grown under normal watering conditions for 18 d before being subjected to a 6-d drought treatment, followed by recovery for 6 d via watering. **B)** Survival rate of each genotype after recovery by rewatering. Values are means ± SD from 4 independent biological replicates (*n* = 100, total plants examined for each genotype). **C)** Fresh weight above ground of each genotype before drought treatment and after recovery by rewatering (*n* = 13). **D, E)** Photosynthetic efficiency **D)** and stomatal conductance **E)** during drought (*n* = 7). **C** to **E)** Boxplots show median (inner thick line) and interquartile range (box). The top and bottom of the box represent the 0.75 and 0.25 percentiles, respectively. The whiskers represent 1.5 times the interquartile range. All the sample points were shown with the

(continued)

brassinazole (BRZ), which diminished BR signaling in *dpy1* plants to a level close to that of WT plants, as verified by the accumulation of phosphorylated SiBZR1 (BRASSINAZOLE-RESISTANT1) (Supplemental Fig. S7A). We then subjected WT (Yugu1), *dpy1*, and BRZ-treated *dpy1* plants to drought stress. After resupplying water, the survival rate of *dpy1* plants increased from $25 \pm 6\%$ to $49 \pm 7\%$ after BRZ treatment, which remained much lower than that of WT plants ($82 \pm 4\%$) (Supplemental Fig. S7, B and C). Furthermore, BRZ treatment partially compensated for the physiological defects of water maintenance and osmoprotectant induction in *dpy1* leaves to various degrees (Supplemental Fig. S7, D to F). We thus propose that the hyperactivation of BR signaling is partially responsible for the increased drought susceptibility of *dpy1*.

SAPK6 acts genetically downstream of DPY1 to regulate plant drought tolerance

Subclass I-type SnRK2s are essential for the acclimation of Arabidopsis to osmotic stress (Soma et al. 2020). We determined that *SAPK6* expression is strongly induced by PEG treatment in foxtail millet (Supplemental Fig. S8A), suggesting that SAPK6 is involved in the osmotic stress response. In a natural population of 916 foxtail millet varieties, we identified 6 major *SAPK6* haplotypes representing over 80% of all varieties, based on public SNP resources (Supplemental Fig. S8B) (Jia et al. 2013). Varieties with different haplotypes displayed substantially different drought tolerance phenotypes in 3 independent field tests. The varieties harboring the *hap5* haplotype showed higher drought tolerance, with a higher relative plant height (drought/normal) than the other varieties (Supplemental Fig. S8C), suggesting that variation at *SAPK6* corresponds with plant drought tolerance in foxtail millet (Supplemental Fig. S8C). Moreover, overexpression of *SAPK6* in foxtail millet resulted in higher drought tolerance at the heading stage compared to the nontransgenic controls (Supplemental Fig. S8D). These results reveal a conserved function for SAPK6 in drought tolerance in foxtail millet.

To investigate the genetic relationship between *DPY1* and *SAPK6* in drought tolerance, we generated *dpy1/Ubipro: SAPK6-3FLAG* (*dpy1/SAPK6-OE*) transgenic plants by overexpressing *FLAG*-tagged *SAPK6* in *dpy1* (Cas9-free *dpy1* knockout generated by genome editing in the Ci846 background) (Zhao et al. 2020). We grew WT (Ci846), *dpy1*, and 2 independent *dpy1/SAPK6-OE* lines in the same pot to ensure

the same severity of soil drying during drought, which we verified by continuously monitoring soil water content and water potential for each genotype (Supplemental Fig. S5). The loss of DPY1 function in the Ci846 background also resulted in plants that were more sensitive to drought, as shown by the lower survival rates of these *dpy1* plants ($7 \pm 4\%$) compared to the WT ($27 \pm 14\%$) (Fig. 4, A and B; Supplemental Fig. S6). In agreement with this finding, the fresh weight of aboveground biomass decreased to a greater extent in *dpy1* ($64 \pm 9\%$) than in WT plants ($35 \pm 14\%$) after rewatering (Fig. 4C). Overexpressing *SAPK6* fully rescued the physiological defects of *dpy1* plants (Fig. 4, A to C).

During the drought period, we monitored the leaf photosynthetic rates and stomatal conductance of each genotype. These values were lower in *dpy1* at the beginning of the drought period and dropped more quickly during drought compared to WT plants (Fig. 4, D and E), suggesting that *dpy1* plants experienced more damage from drought than the WT. When we overexpressed *SAPK6* in *dpy1*, the photosynthetic rate and stomatal conductance remained high during drought (Fig. 4, D and E), demonstrating that *SAPK6* overexpression protected *dpy1* plants from drought-induced damage. Mechanistically, the drought susceptibility exhibited by *dpy1* plants is closely linked to the impaired induction of osmoprotectant metabolite accumulation and impaired maintenance of leaf water content under water deficit conditions. Indeed, *SAPK6* overexpression increased the accumulation of osmoprotectant metabolites and decreased leaf water loss in *dpy1* plants (Fig. 4, F to H), thus enhancing drought tolerance. These findings suggest a possible functional impairment of SAPK6 caused by the loss of DPY1 function during drought stress. Notably, *SAPK6* overexpression did not diminish the hyperactivation of BR signaling in *dpy1* plants and failed to rescue the leaf droopiness caused by the hyperactivated BR signaling in the mutant (Supplemental Fig. S9), suggesting that *SAPK6* acts downstream of *DPY1* specifically in dehydration signaling but not in BR signaling.

To investigate the role of DPY1 in SAPK6-mediated regulation of drought resistance, we compared the performance of *SAPK6* overexpressing lines in the presence or absence of DPY1 under drought conditions. We chose transgenic lines *Ubipro:SAPK6-3FLAG* (*SAPK6-OE*) and *dpy1/Ubipro: SAPK6-3FLAG* (*dpy1/SAPK6-OE*) with the same abundance of SAPK6-3FLAG, as determined by immunoblotting with an anti-FLAG antibody (Supplemental Fig. S10), and subjected them to periods of drought stress, during which all

Figure 4. (Continued)
open circles, and the circles out of the whiskers represent outliers. **F)** Proline accumulation in leaves over the course of drought treatment. The values are means $\pm$ sd from 4 independent measurements (5 leaves per measurement). **G)** OA capability among the different genotypes during drought stress (Days 3 and 4 into drought treatment). OA was determined by the difference in osmotic potential at full turgor between D0 and drought-treated plants (D3 or D4). The values are means $\pm$ sd from 4 independent measurements (5 leaves per measurement). **H)** Relative water content of leaves (the second fully expanded leaf counted from the top) during drought stress ($n = 5$). Different letters indicate significant differences ($P < 0.05$) within each growth condition or time point of drought by 1-way ANOVA with Tukey's multiple comparisons test. The open circles represent sample data points.
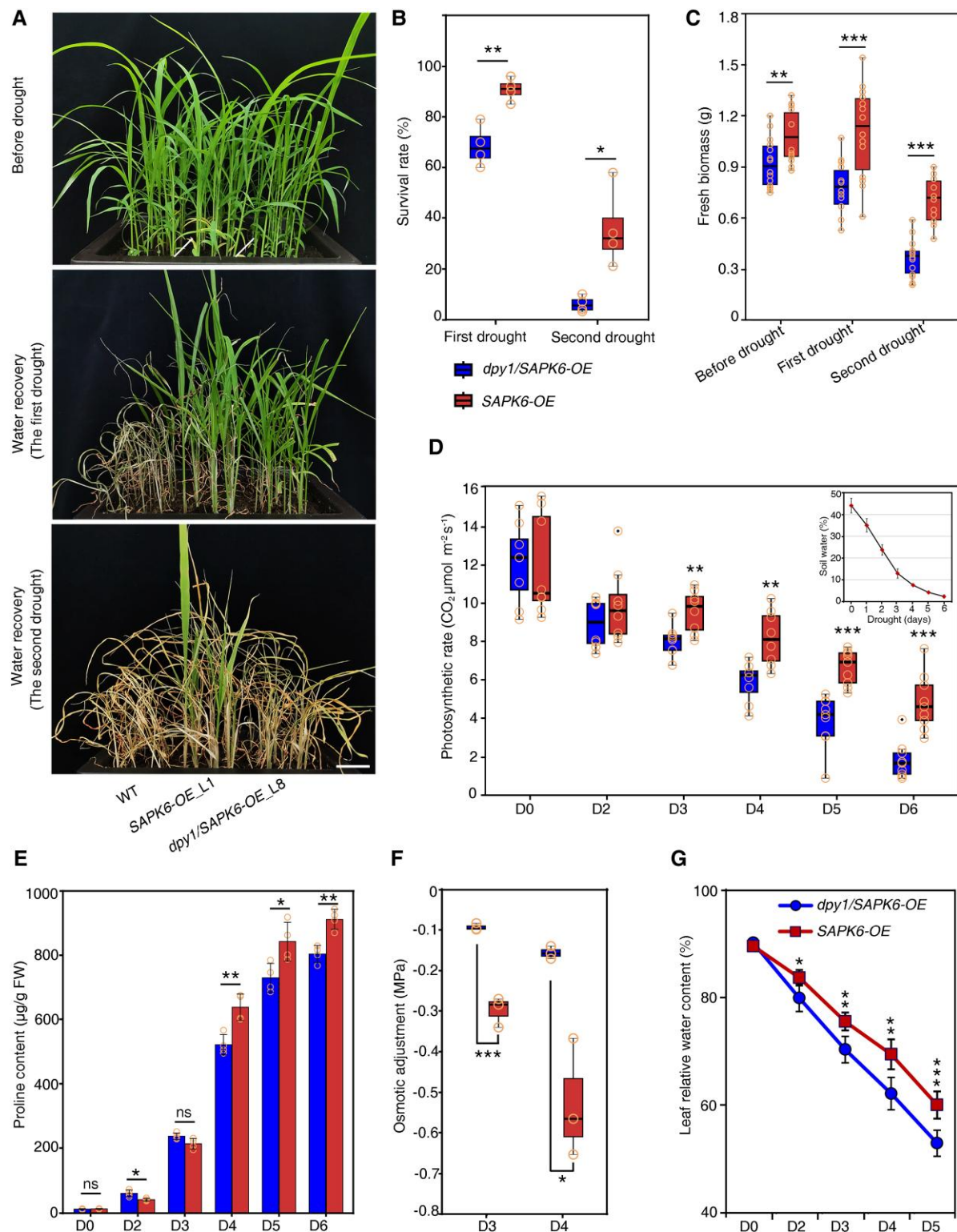
Figure 5. SAPK6-enhanced drought resistance is attenuated in *dpy1* relative to WT plants. **A)** Drought tolerance phenotypes of *SAPK6*-overexpressing plants in the WT and *dpy1* (Ci846) backgrounds after repeated drought treatments. WT (Ci846) plants were used as a control. All plants were grown under normal watering conditions for 18 d before being subjected to a 6-d drought treatment, followed by full recovery via watering (the first drought), after which plants were exposed to an extended drought treatment for 8 d (the second drought). The experiments were repeated 3 times, and representative photographs are shown (Supplemental Fig. S6). Scale bar, 5 cm. **B)** Survival rates, calculated based on 4 replicates (*n* = 104, total plants examined for each genotype). **P < 0.01, *P < 0.05 (Student's *t* test). **C)** Fresh weight of shoots from the indicated genotypes before drought and after recovery via watering (*n* = 13). ***P < 0.001, **P < 0.01 (Student's *t* test). **D)** Photosynthetic performance of

(continued)

plants were exposed to the same severity of drought stress (Supplemental Fig. S5). Notably, *dpy1/SAPK6-OE* plants were much more tolerant to severe drought stress than WT plants (Fig. 5A; Supplemental Fig. S6), while *SAPK6-OE* plants were more drought tolerant than *dpy1/SAPK6-OE* plants, as evidenced by their greater survival rates, higher biomass after drought stress, and more stable photosynthetic rates during the drought period (Fig. 5, A to D). We noticed that osmoprotectant metabolites also accumulated to a greater level in *SAPK6-OE* versus *dpy1/SAPK6-OE* plants (Fig. 5, E and F). The loss of leaf water content occurred more slowly in *SAPK6-OE* plants during drought compared to in *dpy1/SAPK6-OE* plants (Fig. 5G). Taken together, these findings suggest that DPY1 is crucial for SAPK6-mediated regulation of plant drought tolerance.

To validate the above genetic relationship, we performed transcriptome deep sequencing (RNA-seq) analysis of WT, *dpy1*, and *dpy1/SAPK6-OE* plants before and after drought treatment (Supplemental Fig. S11A). We detected 5,818, 6,479, and 7,013 drought-regulated differentially expressed genes (DEGs, with a fold change [FC] > 2.0 and a false discovery rate [FDR] < 0.05) in WT, *dpy1*, and *dpy1/SAPK6-OE* plants, respectively, after a 3-d drought treatment (soil water content dropped to $11.8 \pm 1.6\%$) relative to their well-watered control plants. Of the drought-responsive genes in the WT, approximately one-third (1,542 out of 5,818) were no longer drought responsive in *dpy1* plants (Supplemental Fig. S11B); we designated them as DPY1-dependent drought-responsive genes. Of these 1,542 genes, nearly one-quarter (or 379) recovered their response to drought upon *SAPK6* overexpression (Fig. 6A; Supplemental Fig. S11B and Data Set S2), suggesting that *SAPK6* functions as a downstream target of *DPY1* to regulate the transcriptional response.

We also analyzed gene expression profiles among different genotypes under the same environmental conditions. Under drought conditions, we identified 422 upregulated (SAPK6-activated) and 102 downregulated (SAPK6-repressed) genes from a comparison between *dpy1/SAPK6-OE* and *dpy1* plants (FC > 2.0 and FDR < 0.05) (Fig. 6B; Supplemental Data Set S3). We observed that most of these genes exhibited an opposite regulation trend between *dpy1/SAPK6-OE* versus *dpy1* and *dpy1* versus WT, with a coefficient correlation of -0.23 ($P < 0.001$). Specifically, 226 (54%) out of 422

SAPK6-upregulated genes were repressed, and 70 (69%) out of 102 SAPK6-downregulated genes were induced in *dpy1* relative to WT plants, respectively (Fig. 6C). These findings indicate that the loss of DPY1 function impairs SAPK6-mediated regulation of its downstream genes. However, *SAPK6* overexpression largely returned the overall expression profile of *dpy1* to or even higher than that of the WT (Fig. 6C), suggesting that the overaccumulation of SAPK6 can compensate for the diminished activation of SAPK6 that results from the absence of DPY1. These results suggest that DPY1 and SAPK6 are involved in regulating many common downstream genes and that *SAPK6* acts downstream of *DPY1*.

Gene Ontology (GO) enrichment analysis revealed significant enrichment for biological pathways associated with xyloglucan metabolism, cell wall organization and biogenesis, and response to stress within the identified SAPK6-activated genes (Fig. 6D). Of these genes, we noticed several known drought resistance genes such as *SiCBF2* (*C-REPEAT/DRE BINDING FACTOR 2*)/*SiDREB1C* (*Dehydration-Responsive Element-Binding 1C*) and *SiCBF3*/*SiDREB1A* (Tian et al. 2023); ABA receptor genes *SiPYL6A* (*PYRABACTIN RESISTANCE 1-LIKE 6A*) and *SiPYL6B* (Mega et al. 2019); and peroxidase genes (*SiPRX52*) and genes involved in cutin, suberin, and wax biosynthesis (*PEROXYGENASE 4*) (Bang et al. 2022). *OsCBF2* and *OsCBF3* were recently reported as OsSAPK6-regulated downstream genes during cold stress in rice (Jia et al. 2022); likewise, the genes involved in lignin, cellulose, and xylan deposition during secondary cell wall formation act downstream of SnRK2s in Arabidopsis (Liu et al. 2021). These genes were downregulated in *dpy1* versus WT plants, but their expression levels returned to WT levels or higher when *SAPK6* was overexpressed, based on the above RNA-seq data set (Supplemental Fig. S11C). We confirmed these expression profiles by RT-qPCR analysis (Fig. 6E). These findings suggest that SAPK6 regulates the expression of these genes to help maintain leaf water status and osmoprotectant accumulation, and thus drought tolerance.

Under well-watered conditions, we identified 547 genes that are regulated by SAPK6 from a comparison between *dpy1/SAPK6-OE* and *dpy1* plants (Supplemental Fig. S11, D and E, and Data Set S4); moreover, their expression was misregulated in *dpy1* relative to WT plants (Supplemental Fig. S11F). In

Figure 5. (Continued)
dpy1/SAPK6-OE and *SAPK6-OE* plants during drought. ***$P < 0.001$, **$P < 0.01$ (Student's *t* test). **E)** Proline accumulation in leaves at each time point during the first drought period. The values are means $\pm$ sd from 4 independent measurements (5 leaves per measurement). **$P < 0.01$, *$P < 0.05$, ns, not significant (Student's *t* test). **F)** OA capability of *dpy1/SAPK6-OE* and *SAPK6-OE* plants during drought (Days 3 and 4 into first drought treatment). OA was calculated as the difference in osmotic potential at full turgor between D0 and drought-treated plants (D3 or D4). Three independent measurements (5 leaves per measurement) for each genotype. ***$P < 0.001$, *$P < 0.05$ (Student's *t* test). **G)** Relative water content of leaves (the second fully expanded leaf counted from the top) during the first drought stress treatment ($n = 5$). ***$P < 0.001$, **$P < 0.01$, *$P < 0.05$ (Student's *t* test). **B to D, F)** Boxplots show median (inner thick line) and interquartile range (box). The top and bottom of the box represent the 0.75 and 0.25 percentiles, respectively. The whiskers represent 1.5 times the interquartile range. All the sample points were shown with the open circles, and the circles out of the whiskers represent outliers.
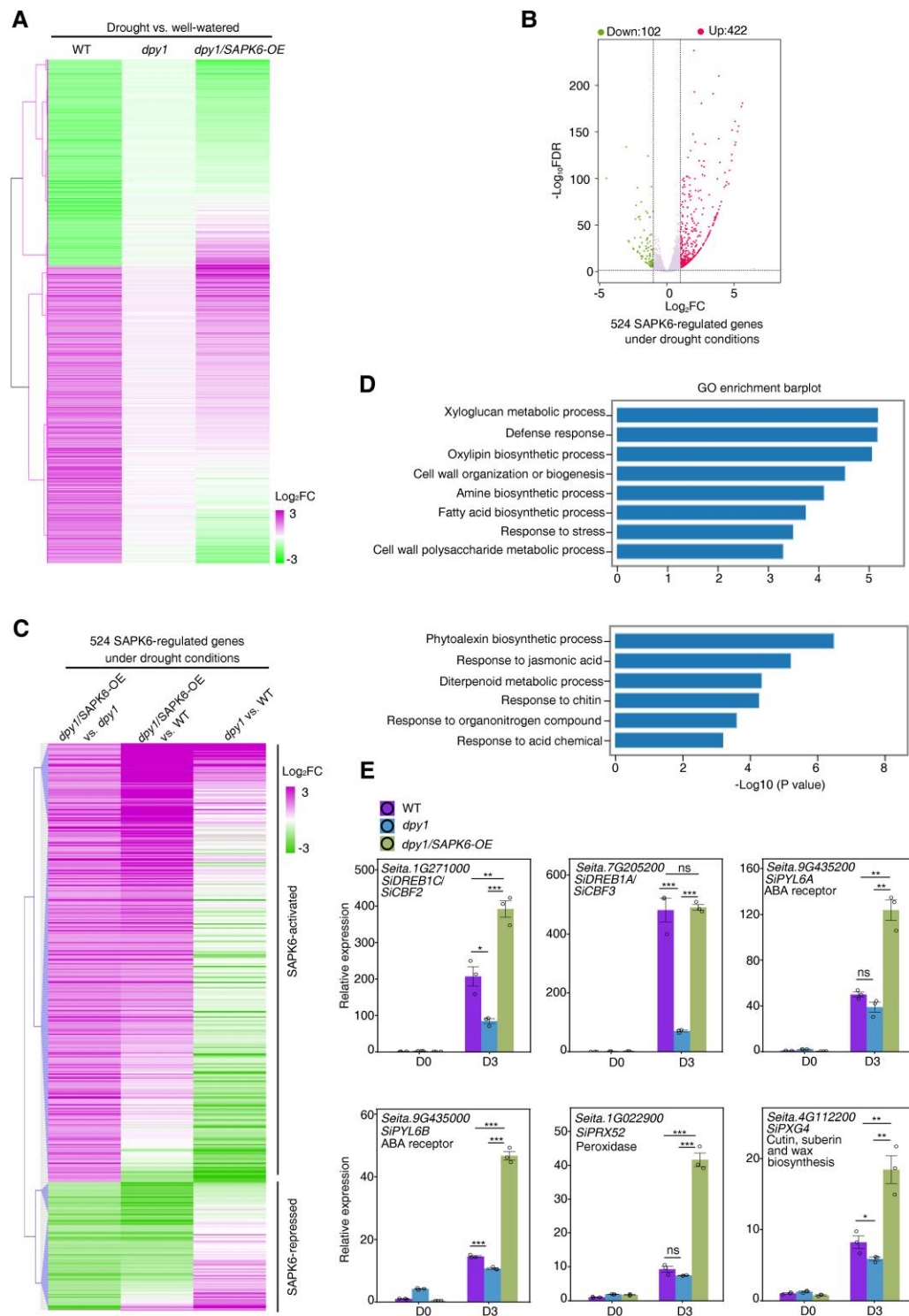
Figure 6. *SAPK6* acts downstream of *DPY1* to modulate gene expression in response to drought. **A)** Hierarchical clustering analysis of the expression of 1,542 DPY1-mediated drought-responsive genes (Supplemental Fig. S11B) in WT, *dpy1*, and *dpy1/SAPK6-OE* plants. **B)** Volcano plots showing DEGs (FC > 2.0, P < 0.05) between *dpy1/SAPK6-OE* and *dpy1* plants under drought conditions. A total of 524 SAPK6-regulated genes were identified, comprising 102 downregulated and 422 upregulated genes in *dpy1/SAPK6-OE* relative to *dpy1* plants. **C)** Hierarchical clustering analysis of the expression of 524 SAPK6-regulated genes under drought conditions in *dpy1/SAPK6-OE* versus *dpy1*, *dpy1/SAPK6-OE* versus WT, and *dpy1* versus WT. **D)** GO analysis of biological pathways enriched in SAPK6-upregulated (upper) or SAPK6-downregulated (lower) genes under drought conditions. **E)** RT-qPCR validation of the expression levels of SAPK6-regulated drought resistance genes in WT, *dpy1*, and *dpy1/SAPK6-OE* plants on D0 and D3. The expression level in D0 WT plants was set to 1.0. The values are means ± SD from 3 biological repeats. P-values were calculated based on Student's *t* test (***P < 0.001; **P < 0.01; *P < 0.05; ns, not significant). Open circles represent sample data points.
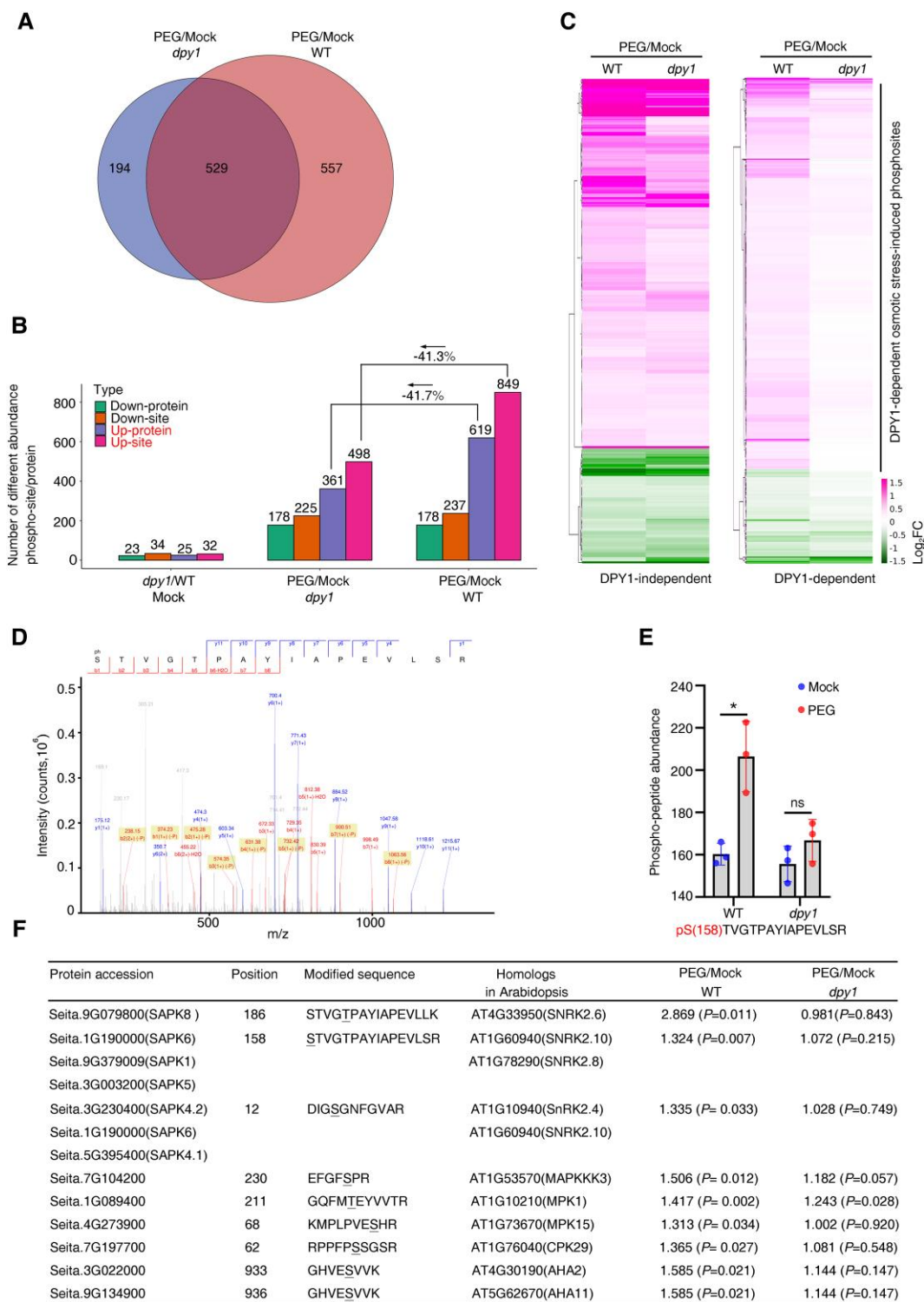
Figure 7. DPY1 is required for osmotic stress–induced global protein phosphorylation. **A)** Venn diagram showing the number of phosphosites with differential phosphorylation levels (FC > 1.3, $P < 0.05$) in WT and *dpy1* plants after osmotic treatment with PEG for 6 h. **B)** Number of upregulated or downregulated phosphopeptides/proteins between the indicated groups. **C)** Heatmap visualizing the direction of regulation for the 529 DPY1-independent and 557 DPY1-dependent osmotic stress–responsive phosphosites in response to osmotic stress in *dpy1* plants compared to WT. A FC (PEG/Mock) > 1.3 ($P < 0.05$) was used as the cutoff. **D)** Mass spectrum derived from high-resolution TMT labeling phosphoproteomics showing a phosphorylated peptide (pSTVGTPAYIAPEVLSR) from endogenous SAPK6. **E)** MS quantification showing the induction of the phosphorylated peptide (pSTVGTPAYIAPEVLSR) in WT and *dpy1* plants after osmotic treatment for 6 h. The values are means ± sd from 3 biological repeats. *P*-values were calculated based on Student's *t* test (*$P < 0.05$; ns, not significant). The solid circles represent sample data points. **F)** List of several DPY1-dependent upregulated phosphosites in response to osmotic stress. The ratio of induction (PEG/Mock) is shown as mean ± sd from 3 biological repeats. *P*-values were calculated based on Student's *t* test.
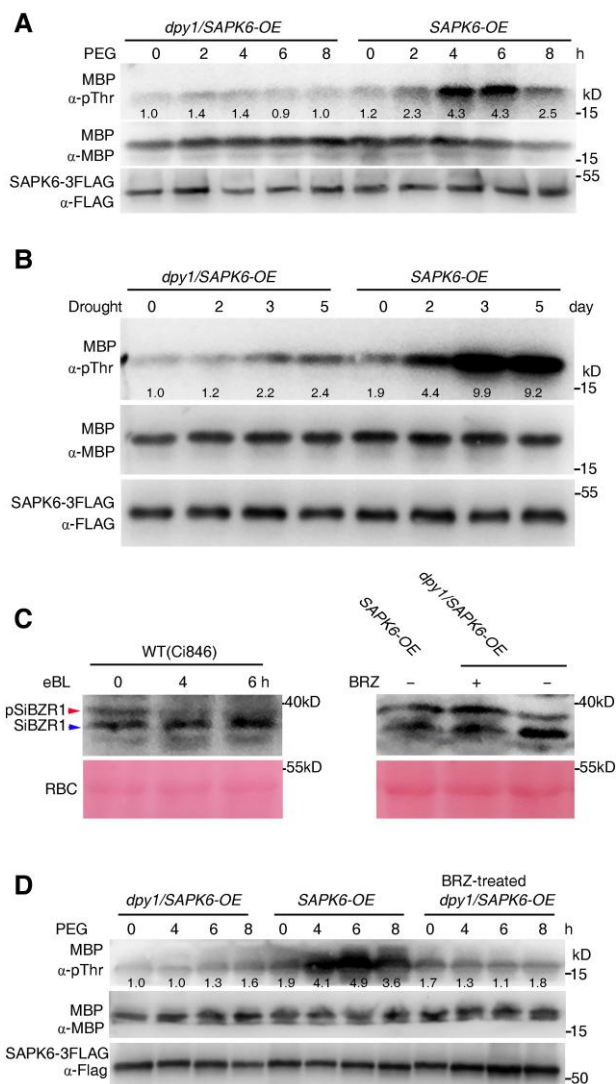
Figure 8. DPY1 is required for SAPK6 activation in response to dehydration stress. **A, B)** SAPK6 kinase activity in *dpy1/SAPK6-OE* and *SAPK6-OE* plants subjected to **A)** short-term osmotic treatment with PEG6000 or **B)** long-term drought treatment. SAPK6-3FLAG was IP from the transgenic plants at the indicated time point. Equal amounts of SAPK6-3FLAG were incubated with MBP as substrate for transphosphorylation to examine SAPK6-3FLAG kinase activity. Phosphorylation of MBP by SAPK6-3FLAG was detected by immunoblotting with an anti-pThr antibody. The input amount of SAPK6-3FLAG or MBP substrate was examined by immunoblotting with an anti-FLAG or anti-MBP antibody, respectively. The ImageJ software was used to quantify signal intensities. **C)** Immunoblots probed with an anti-SiBZR1 antibody in the indicated genotypes treated with epibrassinolide (eBL, left) or BRZ (right), an inhibitor of BR biosynthesis. The blot on the left indicates an increase in the ratio of nonphosphorylated SiBZR1 (blue arrowhead) relative to phosphorylated SiBZR1 (pSiBZR1, red arrowhead) in WT plants due to eBL treatment. The blot on the right indicates a decrease in the level of nonphosphorylated SiBZR1 relative to phosphorylated pSiBZR1 due to BRZ treatment as proof of the reduction in hyperactivated BR signaling in *dpy1/SAPK6-OE* plants. *SAPK6-OE* transgenic plants were used for comparison. Rubisco (RBC) was used as a loading control. **D)** SAPK6

(continued)

addition, two-thirds (or 362) of the 547 SAPK6-regulated genes under normal conditions were not BR responsive by comparison with our previously identified BR-responsive gene in foxtail millet (Zhao et al. 2020) (Supplemental Fig. S11G). Collectively, our findings support the notion that *SAPK6* acts downstream of *DPY1* to synergistically regulate plant drought tolerance in foxtail millet, with minimal contribution from DPY1-mediated BR signaling.

DPY1 is required for global dehydration-induced phosphorylation responses

As DPY1 is an LRR-RLK, we wondered if it might affect global protein phosphorylation in response to drought stress. To explore this possibility, we subjected WT and *dpy1* plants to a short-term PEG treatment (−0.75 MPa) for 6 h, followed by tandem mass tag (TMT) labeling-based quantitative phosphoproteomic analysis before and after PEG treatment (Supplemental Fig. S12, A and B). We identified 12,363 phosphosites in 10,623 unique phosphopeptides corresponding to 4,735 proteins. Of these, 1,086 and 723 phosphosites showed significantly differential phosphorylation levels (FC >1.3; $P < 0.05$) after PEG treatment in WT and *dpy1* plants, respectively, with 529 phosphosites in both genotypes (Fig. 7A). In WT plants, 557 (or 51.3%) of the 1,086 osmotic-responsive phosphosites were DPY1 dependent; they were still present in *dpy1* plants but no longer responded to osmotic stress (Fig. 7A; Supplemental Data Set S5). Moreover, the number of upregulated phosphosites decreased by more than 40% in *dpy1* plants (498 up-sites) compared to WT plants (849 up-sites) in response to osmotic treatment, while the number of downregulated phosphosites was comparable between the 2 genotypes (225 in *dpy1* and 237 in the WT) (Fig. 7B). These findings demonstrate that DPY1 is required for the global phosphorylation response to osmotic stress, supporting the notion that DPY1 plays a critical role in osmotic signal transduction.

We compared the direction of regulation of the 529 DPY1-independent and 557 DPY1-dependent osmotic-responsive phosphosites in response to osmotic stress between WT and *dpy1* plants. The DPY1-independent osmotic-responsive phosphosites showed similar regulation trends in WT and *dpy1* plants in response to osmotic stress. In contrast, the DPY1-dependent osmotic-responsive phosphosites only responded in WT plants and almost lost their responses to
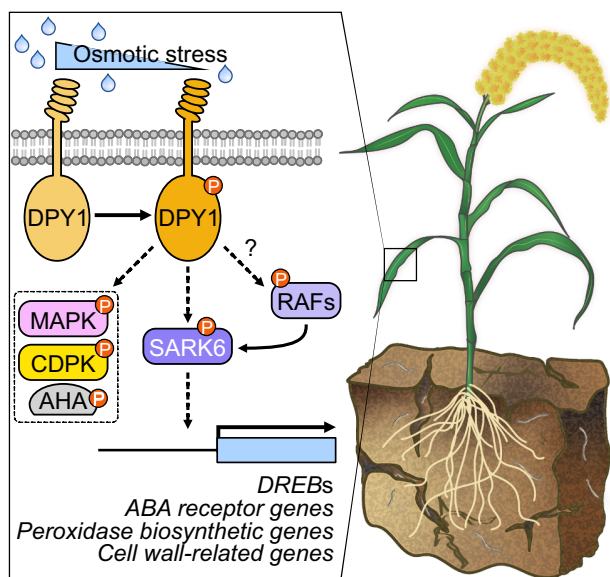
Figure 8. (Continued)
kinase activity from *SAPK6-OE* or *dpy1/SAPK6-OE* plants treated with or without BRZ in response to PEG6000-mediated osmotic stress. *dpy1/SAPK6-OE* plants were pretreated with 5 μM BZR for 6 h to reduce hyperactivated BR signaling and together with nontreated *dpy1/SAPK6-OE* and *SAPK6-OE* plants were subjected to osmotic treatment for the indicated times. The kinase activity of SAPK6-3FLAG was examined as described above. ImageJ was used to quantify signal intensities. All the experiments were repeated twice **C)** or 3 times **A, B, D)** independently with similar results, and 1 representative result is shown.
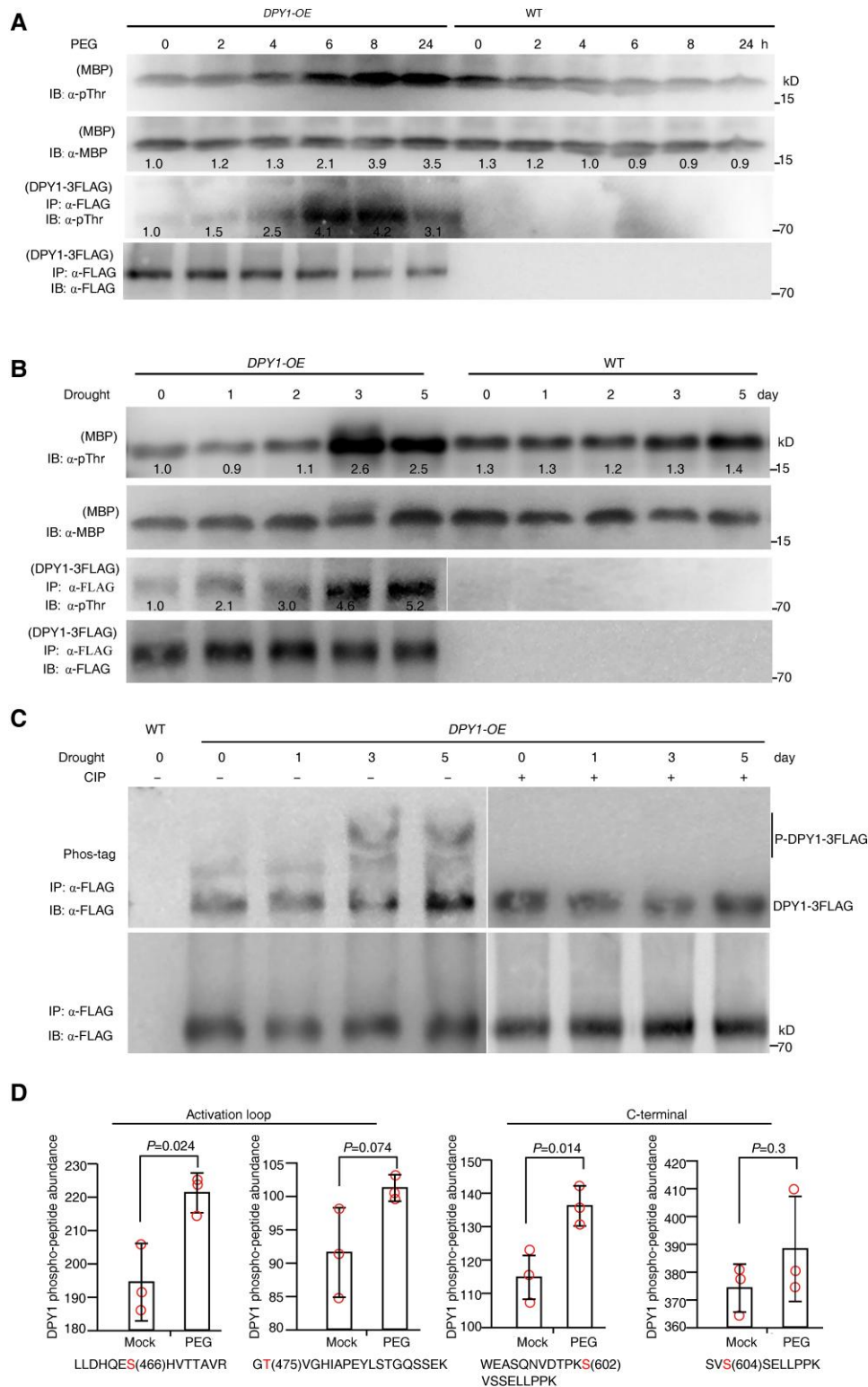
Figure 9. Dehydration stress induces the phosphorylation and activation of DPY1. **A, B)** Short-term osmotic stress (−0.75 MPa) imposed by 20% PEG6000 **A)** or long-term drought stress **B)** treatment raises the phosphorylation level of DPY1 and activates its kinase activity. Transgenic plants harboring *Ubipro:DPY1-3FLAG* (*DPY1-OE*) or WT plants were exposed to 20% PEG6000 **A)** or natural drought stress **B)** for the indicated times. DPY1-3FLAG was IP from the plants with anti-FLAG agarose beads and IB with an anti-pThr antibody to detect the phosphorylation status of DPY1 (lower 2 lanes) or incubated with MBP for the kinase assay to examine DPY1 kinase activity (upper 2 lanes). The input amounts of DPY1-3FLAG for phosphorylation or kinase assays were examined by immunoblotting with an anti-FLAG antibody. The input amounts of MBP were examined by immunoblotting with an anti-MBP antibody. MBP phosphorylation by IP DPY1-3FLAG in the kinase assay was detected by

(continued)

We detected a phosphorylation site at Ser-158 in the SAPK6 peptide STVGTPAYIAPEVLSR (Fig. 7D; Supplemental Fig. S14), which is located within the activation loop of SAPK6 (Supplemental Fig. S14) and was shown to be essential for osmotic stress–induced SnRK2 activation in Arabidopsis (Boudsocq et al. 2007; Vlad et al. 2010). The osmotic stress–induced phosphorylation of Ser-158 was substantially diminished in *dpy1* compared to WT plants (Fig. 7E). These results suggest that DPY1 is required for SnRK2 activation. In addition, we identified several phosphopeptides from other protein kinases, including MAP KINASE KINASE KINASE 3 (MAPKKK3, encoded by Seita.7G104200), MPK1 (Seita.1G089400), MPK15 (Seita.4G273900), and CALCIUM-DEPENDENT PROTEIN KINASE 29 (CPK29, encoded by Seita.7G197700) (Fig. 7F). The accumulation of the phosphopeptides from these kinases decreased in *dpy1* plants compared to WT plants in response to osmotic stress (Fig. 7F), indicating that their kinase activity is likely regulated by DPY1 under osmotic stress.

DPY1 is required for SAPK6 activation in response to osmotic stress

The phosphoproteomic analysis described above revealed that DPY1 is required for phosphorylation of the Ser-158 residue of SAPK6 upon osmotic stress. To explore if osmotic stress–induced SAPK6 activation requires DPY1, we performed an in vitro phosphorylation assay using immunopurified SAPK6 from *dpy1/SAPK6-OE* and *SAPK6-OE* transgenic plants grown under control conditions or treated with PEG solution as a time course. We incubated purified SAPK6-3FLAG bound to agarose beads with myelin basic protein (MBP), a general kinase substrate, to examine SAPK6 activity. SAPK6-3FLAG kinase became active at 4 to 6 h of PEG treatment in WT plants. However, we detected no activity from SAPK6-3FLAG immunopurified from the *dpy1* mutant at any time point (Fig. 8A). Furthermore, the phosphorylation level of SAPK6-3FLAG was much lower in *dpy1* versus WT plants before and during PEG treatment (Supplemental Fig. S15A). We also examined SAPK6-3FLAG kinase activity in response to 6 d of drought stress. SAPK6-3FLAG became progressively activated by drought stress in WT plants, especially after 3 to 5 d of drought treatment, with extremely strong kinase activity compared to the starting time point. In contrast, such activation was much more modest in *dpy1* plants (Fig. 8B). Correspondingly,

Figure 10. Proposed model for DPY1-mediated osmotic stress signaling in foxtail millet. Once plants sense drought stress, DPY1 kinase located at the cell surface is activated, which might be achieved through heterodimerization with unknown RLKs or association with other kinases that are activated after signal initiation. DPY1 modulates the status of at least half of all osmotic stress–induced global phosphosites including MAPK cascades, CDPKs, plasma membrane H⁺-transporting ATPase (AHA), and SnRK2s. SAPK6, a member of subgroup I SnRK2s, acts downstream of DPY1 to transmit osmotic signaling. DPY1 is required for full SAPK6 activation and the regulation of downstream gene expression (e.g. *DREB*s, ABA receptor genes, and cell wall formation–related genes) in response to osmotic stress, thus optimizing plant physiological responses to help acclimate to environmental challenges. Solid and dashed arrows indicate direct and indirect regulation, respectively. Question mark indicates undetermined regulation. The small circles containing P indicate residue phosphorylation.

osmotic stress in *dpy1* plants. Of them, a total of 448 phosphosites were upregulated by osmotic stress, which we designated as DPY1-dependent osmotic stress–induced phosphosites (Fig. 7C). GO enrichment analysis of the DPY1-dependent osmotic stress–induced phosphosites to identify their associated molecular functions revealed that most of the proteins represented by the phosphosites are transporters and kinases (Supplemental Fig. S13). Notably, several phosphosites originated from SnRK2 members.

Figure 9. (Continued)
immunoblotting with an anti-pThr antibody. The phosphorylation of MBP treated with extracts from WT plants represents the basal phosphorylation level. The ImageJ software was used to quantify signal intensities. **C)** Phos-tag assay showing the induction of phosphorylation of DPY1-3FLAG by drought stress. DPY1-3FLAG was IP from plants carrying the *Ubipro:DPY1-3FLAG* transgene (*DPY1-OE*) and subjected to drought treatment for the indicated times, followed by treatment with calf intestinal alkaline phosphatase (CIP) when indicated. **D)** Quantification of phosphopeptides from endogenous DPY1 in WT (Yugu1) seedlings under normal or osmotic stress conditions (20% [*w/v*] PEG6000, −0.75 MPa) for 6 h. The values are derived from the analysis of TMT labeling phosphoproteomics. The values are means ± SD from 3 biological repeats. *P*-values were calculated based on Student's *t* test. The open circles represent sample data points. All the experiments were repeated twice **A, B)** or 3 times **C)** independently with similar results, and 1 representative result is shown.

drought-induced phosphorylation of SAPK6-3FLAG was almost completely abolished in *dpy1* compared to WT plants (Supplemental Fig. S15B). These results confirm the notion that DPY1 is required for osmotic stress/drought-induced SAPK6 phosphorylation and activation.

BR signaling might play an antagonistic role in SnRK2 activation by degrading the kinase BRASSINOSTEROID-INSENSITIVE2 (BIN2), a key inhibitor of BR signaling that was shown to activate SnRK2s directly via phosphorylation in Arabidopsis (Cai et al. 2014). We thus explored whether the hyperactivation of BR signaling in the *dpy1* background might antagonize SAPK6 activation. The phosphorylation status of SiBZR1 was used as a maker for BR signaling output (Fig. 8C). We treated *dpy1/SAPK6-OE* plants with BRZ to decrease BR signaling to a level approaching that of *SAPK6-OE* plants, as verified by a ratio of abundance of nonphosphorylated versus phosphorylated SiBZR1 (Fig. 8C). We then treated these plants with 20% PEG for 8 h. Subsequently, we IP SAPK6-3FLAG with an anti-FLAG antibody for MBP phosphorylation assays as described above. SAPK6 was activated by osmotic stress in *SAPK6-OE* plants, but not in *dpy1/SAPK6-OE* or BRZ-treated *dpy1/SAPK6-OE* plants (Fig. 8D). Moreover, the hyperactivated BR signaling of *dpy1* plants appeared to rapidly decline to WT levels within 4 h in response to PEG treatment, as indicated by the SiBRI1 (BRASSINOSTEROID-INSENSITIVE1) phosphorylation level (Supplemental Fig. S16). Collectively, these findings suggest that hyperactivation of BR signaling in the *dpy1* background does not appreciably affect SAPK6 activation in response to osmotic stress.

Water loss increases DPY1 phosphorylation and activates its kinase activity

DPY1 is a plasma membrane–anchored kinase (Zhao et al. 2020; Wang et al. 2021), and whether and how it responds to external dehydration signals are unknown. We monitored DPY1 kinase activity in plants in response to osmotic stress. First, we confirmed that MBP can be used as an in vitro substrate for DPY1 kinase activity (Supplemental Fig. S17). We then subjected transgenic plants overexpressing *FLAG-tagged DPY1* (*Ubipro:DPY1-3FLAG*) to short-term PEG-mediated osmotic stress or a long-term drought stress treatment, followed by immunoprecipitation of DPY1-3FLAG with an anti-FLAG antibody and in vitro incubation with MBP. Under a time course of PEG treatment, the phosphorylation level of IP DPY1-3FLAG started to increase at the 4-h time point and peaked at 6 to 8 h, as observed by immunoblotting with an anti-pThr antibody (Fig. 9A). In parallel, DPY1 kinase activity was activated at 4 h and remained high thereafter, as revealed by examining the MBP phosphorylation status with an anti-pThr antibody (Fig. 9A).

We obtained similar results in plants exposed to long-term drought treatment, with DPY1-3FLAG showing a marked increase in phosphorylation level, especially at 3 to 5 d of drought treatment. Consistent with this observation, DPY1

kinase activity was also strongly activated at these time points, as indicated by the elevated MBP phosphorylation level (Fig. 9B). Moreover, the DPY1-3FLAG band displayed a change in mobility at 3 to 5 d of drought treatment in a Phos-tag gel (Fig. 9C), which was abolished by treatment with phosphatase (Fig. 9C; Supplemental Fig. S18). These results confirm the notion that DPY1 phosphorylation is induced in response to drought. These findings suggest that osmotic stress increases the phosphorylation and kinase activity of DPY1 in vivo.

To determine the residues in DPY1 that are responsive to osmotic stress, we compared phosphosites derived from DPY1-3FLAG extracted from the transgenic plants before and after PEG treatment. We IP DPY1-3FLAG from plants grown under control conditions (0 h time point) and exposed to PEG for 6 h (as shown in Fig. 9A) and isolated the corresponding protein bands from the gel for analysis by MS. We identified 4 in vivo phosphosites in 3 DPY1-3FLAG peptides (Supplemental Fig. S19A): Thr-475, Thr-599, Ser-602, and Ser-604. Of these, Ser-602, a site specific to DPY1 and absent in related kinases (Supplemental Fig. S19B), was phosphorylated only upon PEG treatment; we detected the remaining phosphosites either under both conditions or only under the control conditions, suggesting that the phosphorylation of Ser-602 might play a key role in regulating DPY1 function in response to stress.

Additionally, we examined changes in the abundance of phosphosites from endogenous DPY1 in response to osmotic stress using the data from TMT-labeled quantitative phosphoproteomics. We identified 4 phosphosites in DPY1 from WT plants: Ser-466, Thr-475, Ser-602, and Ser-604 (Supplemental Fig. S12C), 3 of which (Thr-475, Ser-602, and Ser-604) overlapped with those in detected from the transgenic *DPY1-3FLAG* plants (Supplemental Fig. S19A). The levels of all 4 phosphosites were upregulated upon PEG treatment (Fig. 9D). Taken together, these findings suggest that DPY1 activity and function might be regulated by these residues in response to drought.

DPY1 indirectly regulates SAPK6 kinase activity

Given that DPY1 directly interacts with SAPK6 and is required for SAPK6 activation under osmotic stress, we asked whether DPY1 phosphorylates SAPK6 directly. In vitro kinase assays clearly showed that SiRAF20, a member of the B4 group of kinases, can directly phosphorylate the kinase-dead variant mSAPK6, demonstrating a conserved RAF-SnRK2 cascade across plants. In contrast, DPY1 did not directly phosphorylate kinase-dead mSAPK6 or mSiRAF20 (Supplemental Fig. S20), indicating that DPY1 might require an additional kinase to activate SAPK6 under osmotic/drought stress conditions (Fig. 10).

Discussion

Plants are often exposed to repeated osmotic stress events under natural conditions and must mount the appropriate

acclimatory responses at multiple levels to ensure their survival. Currently, while these responses are well understood at the transcriptional and metabolic levels, changes in protein phosphorylation remain more enigmatic, although thousands of phosphosites change in response to osmotic stress (Lin et al. 2020), representing the basis of osmotic signal transduction. RLKs can sense a wide variety of external and endogenous stimuli to initiate multiple signaling cascades (Osakabe et al. 2013), but the involvement of cell surface RLKs in osmotic stress and whether and how they trigger signal transduction remain unclear.

Here, we linked a member of the LRR-RLK family to osmotic stress signaling in plants (Fig. 10). We showed that 1,086 phosphosites in foxtail millet leaves were regulated by osmotic stress, more than 50% of which were DPY1 dependent (Fig. 7, A to C). These findings are reminiscent of the auxin phosphorylation cascade initiated by the other LRR-RLK TRANSMEMBRANE KINASE 1 (TMK1), with auxin inducing the phosphorylation of over 1,000 sites, 90% of which are TMK1 dependent (Friml et al. 2022). Among DPY1-dependent osmotic stress–induced phosphosites, most are kinases and transporters, including SnRK2s, MAPK cascade kinases, and plasma membrane H+-transporting ATPases (Fig. 7F; Supplemental Fig. S13), which were also identified in the early osmotic stress response of Arabidopsis (Stecker et al. 2014), indicating that they are key early responsive components to osmotic stress across plants.

SnRK2s are activated by various osmotic stresses and are the central kinases of osmotic signaling. Except for RAFs, the kinases upstream of SnRK2s that act during osmotic stress remain largely unknown, although several kinases such as BRI1-ASSOCIATED RECEPTOR KINASE 1 (BAK1) and BIN2 were reported to interact with and phosphorylate SnRK2s to regulate ABA signaling (Shang et al. 2016; Deng et al. 2022). Here, we demonstrated that DPY1 is essential for osmotic stress–induced phosphorylation (especially at Ser-158) (Fig. 7E) and consequent activation of SAPK6 (a member of SnRK2 subclass I) (Fig. 8). This process is likely to require additional kinases to activate SAPK6 because DPY1 interacts with but cannot directly phosphorylate SAPK6 (Supplemental Fig. S20). Therefore, our study connects osmotic stress–induced activation of a member of the SnRK2 family with an LRR-RLK located at the cell surface, which advances our understanding of early osmotic signaling in plants.

In addition to SnRK2 family members, we identified other kinases (such as a MAPKKK and 2 MAPKs) that respond to osmotic stress in a DPY1-dependent manner (Fig. 7F). In yeast, MAPK signaling cascades were shown to act downstream of transmembrane osmosensors to control the global transcriptional response to osmotic stress (Hohmann 2002). In contrast, it remains unclear how MAPK cascades communicate with their upstream components under osmotic stress conditions in plants. Our findings provide clues about how MAPK cascades regulate phosphorylation upon osmotic stress in plants, which requires the RLK DPY1. In addition

to kinases, we detected decreased phosphorylation of some transporters including plasma membrane H+-transporting ATPase (e.g. AHA2 and AHA11) in dpy1 plants in response to osmotic stress (Fig. 7F). A recent study in Arabidopsis showed that ABA can activate BAK1, which in turn phosphorylates and activates AHA2 to trigger ABA-induced stomatal closure and cytoplasmic alkalinization during drought stress, thus enabling plants to acclimate to drought stress (Pei et al. 2022). Given that DPY1 is phylogenetically close to BAK1 (Fig. 2), DPY1 is likely to also be involved in the process.

Based on the localization of DPY1 at the cell membrane and its global influence in the phosphorylation response upon induction by osmotic stress (Supplemental Fig. S3; Fig. 7), we propose that DPY1 is an indispensable component in early osmotic signaling that is required for the phosphorylation cascades emanating from SnRK2s and other signaling pathways. DPY1-related kinases have evolved only in land plants, suggesting that dehydration stress signaling mediated by DPY1 represents an adaptive strategy of these plant species to cope with repeated drought events. These clades of kinases in LRR-RLK II are early signaling components in multiple biological processes, such as plant immunity, BR-mediated plant architecture, stem cell fate determination (Hu et al. 2018; Li et al. 2019; Zhao et al. 2020), and, as determined here, osmotic signaling.

DPY1 can be phosphorylated and activated by dehydration stress (Fig. 9, A to C). Our quantitative phosphoproteomic analysis of endogenous DPY1 also revealed greater phosphorylation at several specific Ser/Thr sites such as S466, T475, S602, and S604 after osmotic stress (Fig. 9D). The first 2 phosphosites (S466 and T475) are located within the activation loop of the DPY1 kinase domain (KD). The other 2 sites (S602 and S604) are located within the most variable C-terminal part of the protein (Supplemental Fig. S19B). In general, phosphorylation in the activation loop is considered to be a conserved mechanism for the activation of protein kinases. In line with this notion, mutating Thr-475 or Ser-466 to Ala discernibly reduced DPY1 autophosphorylation (Wang et al. 2021). However, site-directed mutagenesis of the equivalent residues in Arabidopsis NIK1 revealed a complex role for their phosphorylation in terms of NIK1 kinase activity (Carvalho et al. 2008; Santos et al. 2009). The C-terminus of BRI1 exerts self-inhibition on its kinase activity, and phosphorylation of some residues in the C-terminal region released its inhibitory effect (Wang et al. 2005). Indeed, the S604A mutation diminished DPY1 autophosphorylation (Wang et al. 2021). Whether DPY1 phosphorylation occurs in these residues and is linked to DPY1 activation remains to be tested.

Such a model for the role of DPY1 in plant responses to osmotic stress or drought is reminiscent of the other recently identified LRR-RLK HYDROGEN PEROXIDE-INDUCED CA2+ INCREASE1 (HPCA1), a putative a hydrogen peroxide (H2O2) sensor (Wu et al. 2020). HPCA1 can be oxidized by H2O2 at extracellular cysteine residues within 30 min, leading

to kinase activation and autophosphorylation at intracellular residues and the subsequent activation of Ca^{2+} channels in guard cells (Wu et al. 2020). Compared to HPCA1, several key open questions remain about the mechanism by which DPY1 is activated by osmotic stress. Is DPY1 directly activated by an osmotic stress–induced stimulus (e.g. H_2O_2 or small peptides/molecules) like HPCA1, or is it indirectly activated downstream of other kinases? We consider it unlikely that DPY1 is directly activated by an osmotic stress stimulus for several reasons. First, DPY1 has a very short extracellular domain with only 5 LRR units compared to HPCA1 (10 LRRs) or other classic kinase receptors (e.g. BRI1 [25 LRRs] and FLS2 [28 LRRs]) (Wang et al. 2001; Chinchilla et al. 2007; Wu et al. 2020). Our phylogenetic analysis showed that, together with its Arabidopsis homologs NIKs/CIKs (Hu et al. 2018; Li et al. 2019), DPY1 forms a sister clade with the BAK1/SERK3 subclass of the LRR-RLK II family (Fig. 2). A recent study suggested that CIKs function as coreceptors and help transmit CLAVATA 3 (CLV3) signaling during stem cell maintenance (Hu et al. 2018). Therefore, we propose that DPY1 acts as an assistant component in early osmotic signaling. Second, DPY1 activation and the induction of phosphorylation occur after 4 h of continuous PEG treatment (Fig. 9A). Given that the phosphorylation responses of sensory components occur quickly, usually within minutes (as reported in Arabidopsis), DPY1 activation likely functions downstream of signal initiation, which might be relayed by a second messenger, such as Ca^{2+}. Notably, we identified a calcium-dependent protein kinase (CDPK) as a candidate DPY1-interacting protein (Fig. 1A). How DPY1 is activated needs to be clarified.

With the loss of DPY1 function, plants accumulated insufficient levels of osmoprotectant metabolites and lost more water from their leaves than did the WT, resulting in a greater sensitivity to drought (Figs. 3 and 4). Importantly, the phenotypes observed in *dpy1* plants were rescued by overexpressing *SAPK6*, although SAPK6 was not fully activated by drought (Fig. 8, A and B). A similar phenomenon was previously observed in the BR signaling pathway, as the overexpression of the downstream kinase gene *BR-SIGNALING KINASE 3* (*BSK3*, encoding a receptor-like cytoplasmic kinase) partially rescued the null mutant *bri1-116* lacking function of the BR receptor BRI1 (Zhang et al. 2016). We hypothesize that SAPK6-3FLAG may retain some basal activity in the *dpy1* background due to autophosphorylation or transphosphorylation by other unknown kinases. In fact, we detected phosphorylated SAPK6-3FLAG in the *dpy1* background, although its phosphorylation did not respond to drought stress (Supplemental Fig. S15B). Nevertheless, DPY1 function was still required for SAPK6-mediated protection against drought, as indicated by the attenuation of SAPK6-enhanced drought tolerance in *dpy1* plants compared to WT plants (Fig. 5).

Our genetic evidence therefore places *SAPK6* downstream of *DPY1* in the drought response, which was further supported by RNA-seq analysis. Gene coexpression analysis suggested that *SAPK6* is a downstream target of *DPY1* to

regulate the transcriptional response (Fig. 6A). We thus established a DPY1-SAPK6 signal cascade that is activated by the osmotic stress–triggered phosphorylation to reprogram the downstream transcriptional responses, which is reminiscent of the HK-MAPK signaling cascade in yeast that controls gene expression in response to osmotic change (Hohmann 2002). Like subclass III SnRK2s, subclass I SnRK2s were found to regulate gene expression by changing their downstream substrate activity via phosphorylation. For instance, they were recently shown to phosphorylate VARICOSE (VCS), an mRNA decapping activator, to regulate mRNA decay, ensuring appropriate changes in mRNA populations under osmotic stress in Arabidopsis (Soma et al. 2017). We determined that SAPK6 induced the expression of 422 genes under drought stress, representing approximately 4 times the number of repressed genes (Fig. 6B), while the number of DEGs was comparable upon *SAPK6* overexpression under normal conditions (Supplemental Fig. S11D). This result demonstrates a mainly activating role for SAPK6 in controlling gene expression under drought conditions, similar to the transcriptional activation of ABA-activated subclass III SnRK2s via ABA RESPONSIVE ELEMENT-BINDING FACTOR (ABF) transcription factors (Soma et al. 2020).

Among the SAPK6-activated genes, those involved in cell wall formation were enriched (Fig. 6, D and E). A recent study in Arabidopsis showed that the ABA-activated subclass III SnRK2s induce the expression of genes related to secondary cell wall and lignin deposition by directly activating NAC SECONDARY WALL THICKENING PROMOTING FACTOR1 (NST1), a master transcription factor in this pathway, and that the contents of cell wall components were reduced in the *snrk2.2 snrk2.3 snrk2* mutant (Liu et al. 2021). Indeed, most cell wall components including lignin were also present at lower levels in *dpy1* plants compared to the WT. This might result in the formation of a weaker barrier against evaporation and lead to more water loss through transpiration in response to drought (Bang et al. 2022), resulting in the drought susceptibility of *dpy1* plants. We propose that SAPK6 largely compensates for the drought susceptibility of *dpy1*, at least partially by modulating the composition of the cell wall under drought. In addition, genes encoding *DREB* transcription factors and ABA receptors were also regulated by SAPK6 under drought conditions (Fig. 6E). Like Arabidopsis subclass III SnRK2s, SAPK6 may transcriptionally activate multiple downstream pathways to optimize plant physiological responses to severe drought stress.

We previously showed that loss of DPY1 function led to the hyperactivation of BR signaling (Zhao et al. 2020), which might antagonize the activation of SAPK6 and its downstream genes under drought stress, as BRs might block the activation of SnRK2s by BIN2 by destabilizing the latter (Cai et al. 2014). However, our findings suggest that elevated BR signaling cannot antagonize SAPK6 activation in the *dpy1* background based on 3 lines of evidence. First, decreasing the elevated BR signaling in the *dpy1* background to a WT level using the BR biosynthesis inhibitor BRZ failed to recover

SAPK6 activation in response to osmotic stress (Fig. 8, C and D). Second, the hyperactivated BR signaling in *dpy1* quickly declined to close to the WT level upon osmotic stress (Supplemental Fig. S16). Consistent with this, several studies have showed that BR signaling is greatly inhibited in response to drought/dehydration, as evidenced by the destabilization of the dephosphorylated BRI1-EMS-SUPPRESSOR1 (BES1) (Chen et al. 2017; Nolan et al. 2017). This suggests that BR signaling must be downregulated to reduce growth and acclimate to drought tolerance. As a result, it is unlikely that SAPK6-regulated downstream genes under drought are greatly influenced by DPY1-mediated BR signaling (Fig. 6C). Third, SAPK6 is not implicated in the BR pathway, as *SAPK6* overexpression failed to rescue the leaf droopiness of *dpy1* plants, a phenotype of hyperactive BR signaling (Supplemental Fig. S9), and nearly 70% of all SAPK6-regulated downstream genes under normal conditions were not BR responsive (Supplemental Fig. S11G). However, hyperactivated BR signaling contributed to the drought susceptibility displayed by *dpy1* plants presumably by reducing deposition of lignin and other cell wall components in leaves as previously reported (Bang et al. 2022). Indeed, *SiBZR1* overexpression partially mimics the droopy leaf phenotype seen in *dpy1* and also reduces drought tolerance in foxtail millet (Zhao et al. 2021). Furthermore, reducing elevated BR signaling of the *dpy1* mutant partially compensated for the observed physiological defects of *dpy1* in response to drought as well as its drought-sensitive phenotype (Supplemental Fig. S7).

Setaria species, including foxtail millet and its wild ancestor (*Setaria viridis*), have long been proposed as an ideal system for genetic studies, especially for studying C4 photosynthesis and stress biology (Brutnell et al. 2010; Diao et al. 2014), but there is less experimental support for the notion. Here, we provided a case study showing the great potential of the *Setaria* system for dissecting complex signaling networks. Our identification of the DPY1-SAPK6 signaling module advances our understanding of osmotic signaling in plants and provides candidate targets for the genetic improvement of grain crops in the future.

Materials and methods

Plant materials and growth conditions

Foxtail millet (*S. italica*) variety Yugu1, Ci846, *dpy1* mutant (Yugu1 or Ci846 background), and transgenic plants *dpy1*/DPY1pro:DPY1-GFP and Ubipro:DPY1-3FLAG (Yugu1 background) were used in our previous studies (Zhao et al. 2020). Ubipro:SAPK6-3FLAG and dpy1/Ubipro:SAPK6-3FLAG (Ci846 background) plants were generated in this study. Full-length coding region of SAPK6 was amplified from the total cDNA of Ci846 and then subcloned into a modified binary vector *pTCK303* between *BamHI* and *SpeI* site with 3 repeats of FLAG tags downstream of the insertion (Zhao et al. 2020). The resultant construct was transformed into the

callus of Ci846 or *dpy1* plants, a Cas9-free *dpy1* knockout line generated by genome editing in the Ci846 background (Zhao et al. 2020). More than 15 independent lines were obtained for each, and representative T2 lines were used for subsequent analysis.

All of the plants were grown in greenhouse equipped with T5 4000K fluorescent tubes (Philips) under a long-day condition (16-h light at 28 °C and 8-h dark at 24 °C) at a light intensity of 100 mmol m^{-2} s^{-1}. We imposed a severe drought stress treatment on foxtail millet to distinguish the drought resistance ability among different genotypes. Briefly, all the plants were grown in the same pot with a 3:1 mixture of nutrient soil and roseite under a regular condition for 18 d and then subjected to drought stress with 6 d of withholding water (the first drought), followed by full recovery via watering (Supplemental Fig. S5). To further compare drought resistance, the *dpy1/Ubipro:SAPK6-3FLAG* and *Ubipro:SAPK6-3FLAG* plants additionally underwent an extended drought treatment for 8 d (the second drought). Soil water content and water potential were carefully monitored for each genotype of plants with WP4C Depoint PotentiaMeter (Decagon Devices, USA) and portable soil moisture sensor (LANENDE, China) during a drought period, respectively. For PEG treatment, plants were grown in a small petri dish with moistened filter paper for 7 d and then covered with a thin layer of 20% PEG6000 (−0.75 MPa) solution for several hours, during which the petri dish was constantly shaken to keep the seedlings in full contact with air to protect against possible hypoxia. The seedlings with root removed were immediately harvested for each experiment. Water potential of the 20% (w/v) PEG6000 solution is measured by a freezing point osmometer (Astori Tecnica, Italy) at room temperature.

Measurements of CO$_2$ exchange, proline content, OA, and leaf water content

Gas exchange measurements were conducted in the second fully expanded leaves from the top of each genotype with LI-6800 Portable Photosynthesis System (Li-Cor, USA). Leaves were first equilibrated at a photon density flux of 500 μmol m^{-2} s^{-1} for at least 5 min, and then photosynthesis was measured with a photon density flux of 1,000 μmol m^{-2} s^{-1} and 400 μmol s^{-1} CO$_2$ around the leaf. For proline content measurements, approximately 0.1-g leaves were collected and homogenized in 1 mL of 3% sulfosalicylic acid and centrifuged, and resulting supernatant was incubated with ninhydrin reagents (Suzhou Geruisi Biotechnology Co., Ltd., Suzhou, China). Absorbance values were measured with a Varioskan LUX Multimode Microplate Reader (Thermo Fisher Scientific, USA). OA measurement was performed based on the rehydration method as previously reported (Turner 2018). The leaves at the D0 or dehydrated for 3 or 4 d were excised from plants and soaked with water in the dark for more than 8 h for full rehydration. The turgid leaves were frozen in liquid

nitrogen and then stored at −80 °C. The frozen leaf samples were thawed, and cell sap was pressed from the leaves and subsequently analyzed for osmotic potential using the freezing point osmometer (Astori Tecnica, Italy). OA was calculated as the difference in osmotic potential between nonstressed and stressed leaves of each genotype of plants. Leaf relative water content (LRWC) was determined according to the following formula: LRWC = (fresh weight − dry weight)/(turgid weight − dry weight). The second fully expanded leaves from the top of each genotype were excised for the measurements.

Measurement of endogenous ABA concentration
Approximately 200-mg (fresh weight) plant tissues were homogenized under liquid nitrogen, weighted, and extracted for 24 h with methanol and [^{2}H$_6$]-ABA. Endogenous ABA was purified and measured as previously described (Fu et al. 2012) with some modifications in detection conditions. LC−MS/MS analysis was performed on a UPLC system (Waters) coupled to the 6500 Qtrap system (AB SCIEX). LC separation used a BEH C18 column (1.7 μm, 100 × 2.1 mm; Waters) with mobile phase A 0.05% (*v/v*) acetic acid in water and mobile phase B 0.05% (*v/v*) acetic acid in acetonitrile. The gradient was set with initial 20% B and increased to 70% B within 6 min. ABA was detected in multiple reaction monitoring (MRM) mode with transition. The MRM transitions for ABA and [^{2}H$_6$]-ABA are 263.0 > 153.1 and 269.2 > 159.2. Five plants were collected for each sample, and 3 biological replicates were analyzed for each treatment.

Brassinolide and BRZ treatment
WT and *dpy1/Ubipro:SAPK6-3FLAG* (*dpy1/SAPK6-OE*) seedlings were grown in petri dishes with moistened filter paper for 7 d and then soaked in 5 μM brassinolide (BL) or BRZ solution for 6 h. The BRZ-treated *dpy1/Ubipro:SAPK6-3FLAG* plants, together with nontreated *dpy1/Ubipro:SAPK6-3FLAG* and *Ubipro:SAPK6-3FLAG* plants, were covered with a thin layer of 20% PEG6000 (−0.75 MPa) solution for several hours with constant shaking. These seedlings with root removed were harvested for kinase assay. To evaluate the effect of elevated BR signaling in *dpy1* plants on plant drought resistance, *dpy1* plants grown in soil were sprayed with 1 μM BRZ solution twice a week before exposed to drought stress, during which *dpy1* and WT plants sprayed with water were used as controls.

Subcellular location and BiFC assay
For protoplast transient expression, the full-length coding region of *DPY1* and *SAPK6* was fused in-frame with GFP tag of transient expression vector to generate *35Spro:DPY1-GFP* and *35Spro:SAPK6-GFP*. Primers used for plasmid construction are listed in Supplemental Data Set S6. The constructs (10 μg each) were transformed into protoplasts prepared from 10-d-old foxtail millet leaves as previously reported (Zhao et al. 2020). Before GFP signal observation, the protoplasts expressing DPY1-GFP or SAPK6-GFP were treated with or without 10% PEG6000 for 30 min to investigate osmotic stress possible effects on the protein subcellular location.

For subcellular location observation in stable transgenic plants, the transgenic plants including *dpy1/DPY1pro: DPY1-GFP*, *dpy1/Ubipro:SAPK6-3FLAG*, and *Ubipro: SAPK6-3FLAG* were subjected to drought for 3 d or not. The epidermal cells from leaf blades of *dpy1/DPY1pro: DPY1-GFP* were observed under a confocal fluorescence microscope (Leica TCS SP7, Germany; GFP fluorescence was excited with a 488-nm laser line at a laser intensity of 20% and 765 multiplication gain, and emission was collected through a 510/550-nm filter) to monitor DPY1-GFP signals. Nuclear and cytoplasmic fraction separation for *dpy1/Ubipro:SAPK6-3FLAG* or *Ubipro:SAPK6-3FLAG* transgenic plants was performed as previously reported (Yang et al. 2016). Antihistone H3 (1:5,000, Cell Signaling Technology, Cat. No. 9715) and antitubulin (1:5,000, Cell Signaling Technology, Cat. No. 2144) antibodies were used as nuclear and cytosolic markers, respectively.

For BiFC assay, the coding region of *DPY1* and *Seita.1G023400* was fused in-frame into the C-terminal of truncated YFP in *p2YC* vector to generate *DPY1-cYFP* and *Seita.1G023400-cYFP*, respectively. *SAPK6* coding region was cloned into the N-terminal of truncated YFP in *p2YN* vector to generate *SAPK6-nYFP*. The resultant constructs and control blank vector (cYFP and nYFP) were transformed into Agrobacterium (*Agrobacterium tumefaciens*) strain GV3101 and infiltrated into *N. benthamiana* leaves for 3 d. The fluorescence signal was detected under a confocal fluorescence microscope (Leica TCS SP7) with the excitation wavelength at 514 nm under the laser intensity of 20%. For each combination, at least 10 images were captured under the same exposure settings. The mean fluorescence intensity was calculated by computing integrated density/area using the ImageJ software.

LC−MS/MS analyses of DPY1-3FLAG and Co-IP assay
For identification of DPY1-interacting proteins in plant, 1.5-g fresh leaves were collected from the 3-wk-old *Ubipro: DPY1-3FLAG* transgenic plants and WT plants, respectively. The samples were ground to fine powder with liquid nitrogen and then incubated with the immunoprecipitation buffers (50 mM Tris-HCl, pH 7.6, 150 mM NaCl, 10% glycerol, 0.1% NP-40, 1% Triton X-100, and 1× Complete Protease Inhibitor Cocktail) for extraction of total soluble proteins. The resultant supernatant was incubated with Anti-FLAG M2 Affinity Gel (Sigma-Aldrich, Cat. No. A2220) for enrichment of DPY1-3FLAG protein. IP products were extensively washed and then eluted with 3× FLAG peptide (Sigma-Aldrich, Cat. No. 4799). The eluted proteins were sent to Beijing Qinglian Biotech Co., Ltd., for mass spectrometric analysis. Briefly, the eluted protein solution was separated by SDS−PAGE, and the gel containing coimmunoprecipitated proteins with DPY1-3FLAG was isolated and digested by trypsin. The resultant peptides were separated using a Thermo Scientific EASY-nLc 1000 System.

The raw data were processed using MaxQuant software with the settings as previously reported (Ji et al. 2018). The outputs were searched against the foxtail millet proteome database (https://www.ncbi.nlm.nih.gov/genome/10982). The proteins whose abundance intensity values are 0 in WT plants, which was used as a systemic control, are regarded as the high-confidence DPY1-interacting proteins (Supplemental Data Set S1).

For the Co-IP experiment, the construct *35Spro:SAPK6-GFP* was transiently expressed in the mesophyll protoplasts of *Ubipro:SAPK6-3FLAG* transgenic plants as previously reported (Zhao et al. 2020). The protoplasts were then incubated with the immunoprecipitation buffers (50 mM Tris-HCl, pH 7.6, 150 mM NaCl, 10% glycerol, 0.1% NP-40, 1% Triton X-100, and 1× Complete Protease Inhibitor Cocktail) for extraction of total soluble proteins. SAPK6-GFP protein was IP with GFP-Trap magnetic beads (gtma-20, ChromoTek). The immunoprecipitates were separated on a 10% SDS–PAGE and immunoblotted (IB) with anti-GFP (1:2,000, Abcam, ab6663) or anti-FLAG (1:3,000, Sigma-Aldrich, A8592) antibody. The protoplasts containing empty GFP vector were used as a negative control.

Yeast 2-hybrid assay

Yeast 2-hybrid assays were performed using a split-ubiquitin–based yeast 2-hybrid system (Dualsystems Biotech) to detect the interaction between DPY1 and SAPK6. The *DPY1* coding region without a signal peptide (aa: 30-633) was subcloned into *pBT3-SUC* vector between double *SfiI* sites to generate *DPY1-Cub*, and the full-length *SAPK6* coding region was subcloned into *pPR3-C* vector at the *EcoRI* site to generate *SAPK6-NubG*. Primers used for plasmid construction are listed in Supplemental Data Set S6. The resultant constructs were transformed into the yeast (*S. cerevisiae*) strain NMY51. The yeast strain with 10-fold dilution was grown on SC/−Leu/−Trp or SC/−Leu/−Trp/−His/−Ade medium for 3 d.

PD assay

The sequence encoding KD of *DPY1* (aa: 280-633) and full-length coding region for *SAPK6* were shifted into *pET-28a* (Novagen) between *EcoRI* and *HindIII* site and *pGEX-4T-1* (GE Healthcare) between *EcoRI* and *SalI* site to generate *His-DPY1-KD* and *GST-SAPK6*, respectively. The resultant constructs were expressed in the *Escherichia coli* BL21 (DE3) strain. For the PD assay, about 1.0 μg His-DPY1-KD was incubated with GST-SAPK6 or GST tag protein at 28 °C for 30 min, and GST-SAPK6 and GST protein were collected with GST beads and then washed with 1× PBS at least 5 times. The PD proteins were separated on a 10% SDS–PAGE gel and detected with immunoblotting using an anti-His (1:3,000, Cell Signaling Technology, Cat. No. 12698) or anti-GST (1:3,000, Cell Signaling Technology, Cat. No. 2624) antibody.

In vitro kinase assays

The kinase assays that examined transgenic DPY1-3FLAG and SAPK6-3FLAG kinase activity were performed according to previously reported with some modifications (Belin et al. 2006). Briefly, plants overexpressing DPY1-3FLAG or SAPK6-3FLAG were treated with 20% PEG6000 solution (−0.75 MPa) or drought, respectively. The leaves were ground to fine powder with liquid nitrogen and then incubated with the immunoprecipitation buffers plus 1× Phosphatase Inhibitor Cocktail for extraction of total soluble proteins. The resultant supernatant was incubated with Anti-FLAG M2 Affinity Gel (Sigma-Aldrich, Cat. No. A2220) for enrichment of the flag-tagged protein. Kinase assays were performed by incubation of the IP DPY1-3FLAG or SAPK6-3FLAG with 15 ng MBP substrate protein (Millipore, Cat. No. 13-104) in a total volume of 50 μL kinase buffer (50 mM HEPES [pH = 7.4], 10 mM Mgcl₂, 1 mM DTT, and 1 μM ATP) at 30 °C for 2 h. The reactions were stopped by adding 50 μL 2× SDS buffer. MBP protein phosphorylation analysis was performed by 10% SDS–PAGE separation and IB with anti-pThr antibody (1:5,000 dilutions, Cell Signaling Technology, Cat. No. ab9381). The loading amounts of MBP and DPY1-3FLAG or SAPK6-3FLAG proteins were determined by immunoblot analysis with anti-MBP (1:2,000 dilutions, Sigma-Aldrich, MAB386) and anti-FLAG (1:3,000 dilutions, Sigma-Aldrich, A8592) antibody, respectively. Phosphorylation analysis of IP DPY1-3FLAG and SAPK6-3FLAG was performed by immunoblot with anti-pThr antibody or biotin-pendant Phos-tag (Wako, BTL-111) or by separation in an 8% SDS–PAGE gel supplemented with 100 μM Phos-tag (Wako, 300-93523).

For transphosphorylation analysis among DPY1, SAPK6, and SiRAF20, the sequences encoding KD of DPY1 (aa: 280-633) and SiRAF20 (aa: 927-1199) were cloned into the vector *pGEX-4T-1* between *EcoRI* and *SalI* site to generate *GST-DPY1* and *GST-SiRAF20*. To generate kinase-dead forms of SiRAF20 and SAPK6, site-directed mutagenesis was introduced by overlap PCR to generate *GST-SiRAF20$^{D1086A-G1088A}$* (*mSiRAF20*) and *GST-SAPK6^{K33N}* (*mSAPK6*). Primers used for plasmid construction are listed in Supplemental Data Set S6. The purified proteins from *E. coli* were incubated in a total volume of 50 μL kinase buffer at 30 °C for 2 h. The protein samples were then separated by SDS–PAGE, and protein phosphorylation was determined by immunoblot analysis using biotin-pendant Phos-tag (Wako, BTL-111).

Immunoblot analysis of SiBZR1 and SiBRI1

BL- or BRZ-treated plants as described above were ground to fine powder with liquid nitrogen. 2× SDS sample buffer (0.125 M Tris-HCl, pH 6.8, 4% SDS, 20% glycerol, 2% β-mercaptoethanol, and bromophenol blue) was added. After heating at 95 °C for 5 min, the mixture was centrifuged at 4 °C 12,000 × g for 5 min, and the supernatant was used for SDS–PAGE and immunoblot analysis with anti-SiBZR1 antibody (1:2,000 dilutions) as we previously reported

(Wang et al. 2021). The full coding region of *SiBZR1* was cloned into vector *pET-28a* (Novagen) between *EcoRI* and *HindIII* site to generate His-SiBZR1, and the purified His-SiBZR1 was used to produce the anti-SiBZR1 antibody in a rabbit.

For endogenous SiBRI1 detection, 7-d-old WT and *dpy1* seedlings treated with 20% PEG solution or not were ground to fine powder with liquid nitrogen and then incubated with the immunoprecipitation buffers plus 1× Phosphatase Inhibitor Cocktail for extraction of total soluble proteins. The resultant supernatant was IP with anti-SiBRI1 antibody as we previously reported (Zhao et al. 2020). The sequence encoding the extracellular domain of SiBRI1 (aa: 110-347) was cloned into vector *pET-28a* (Novagen) between *EcoRI* and *HindIII* site to generate His-SiBRI1, and the purified His-SiBRI1 was used to produce the anti-SiBRI1 antibody in a rabbit. The IP SiBRI1 was detected with immunoblot using anti-pThr antibody (1:2,000 dilutions, Cell Signaling Technology, Cat. No. ab9381) or anti-SiBRI1 antibody (1:1,000 dilutions), respectively.

Determination of in vivo phosphorylation sites in transgenic DPY1-3FLAG by LC–MS/MS

The transgenic plants overexpressing DPY1-3FLAG were treated with 20% PEG6000 solution (−0.75 Mpa) for 6 h or not, and then DPY1-3FLAG was IP with anti-FLAG beads and separated by SDS–PAGE. Gels were stained with Coomassie brilliant blue and the DPY1-3FLAG bands were excised for phosphorylation site analysis. Briefly, gel pieces were digested by trypsin, and then the peptides inside were extracted and analyzed by a LC–MS/MS (nanoLC-QE) system equipped with Q Exactive (Thermo Fisher Scientific, USA) coupled to an Easy-nLC 1000 (Thermo Fisher Scientific, USA). MS/MS spectra were searched against DPY1 protein sequence using MASCOT algorithm (v.2.2, Matrix Science).

Phosphoproteomic analysis

WT (Yugu1) and *dpy1* plants were grown in roseite supplemented with Hoagland culture solution for 7 d and then treated with 20% PEG6000 solution (−0.75 MPa) or water (Mock) for 6 h. For each group, a total of 1 g fresh shoots were collected for phosphoproteomic analysis by PTM Biolab LLC. Briefly, (i) sample was first ground with liquid nitrogen and then the powder was transferred to a 5-mL centrifuge tube and sonicated 3 min on ice using a high-intensity ultrasonic processor (Scientz) in lysis buffer (including 1% Triton X-100, 10 mM dithiothreitol, 1% protease inhibitor cocktail, 2 mM EDTA, and 1% phosphatase inhibitor for phosphorylation.). An equal volume of Tris-saturated phenol (pH 8.0) was added. Then, the mixture was further vortexed for 5 min. After centrifugation (4 °C, 10 min, 5,000 × g), the upper phenol phase was transferred to a new centrifuge tube. Proteins were precipitated by adding at least 4 volumes of ammonium sulfate–saturated methanol and incubated at

−20 °C for at least 6 h. After centrifugation at 4 °C for 10 min, the supernatant was discarded. The remaining precipitate was washed with ice-cold methanol, followed by ice-cold acetone for 3 times. The protein was redissolved in 8 M urea and the protein concentration was determined with BCA kit according to the manufacturer's instructions. (ii) The sample was slowly added to the final concentration of 20% (m/v) TCA to precipitate protein and then vortexed to mix and incubated for 2 h at 4 °C. The precipitate was collected by centrifugation at 4,500 × g for 5 min at 4 °C. The precipitated protein was washed with precooled acetone 3 times and dried for 1 min. The protein sample was then redissolved in 200 mM TEAB and ultrasonically dispersed. Trypsin was added at 1:50 trypsin-to-protein mass ratio for digestion overnight. The sample was reduced with 5 mM dithiothreitol for 60 min at 37 °C and alkylated with 11 mM iodoacetamide for 45 min at room temperature in darkness. Finally, the peptides were desalted by Strata × SPE column. Tryptic peptides were firstly dissolved in 0.5 M TEAB. Each channel of peptide was labeled with their respective TMTpro reagent (based on manufacturer's protocol, Thermo Scientific) and incubated for 2 h at room temperature. Five microliters of each sample was pooled, desalted, and analyzed by MS to check labeling efficiency. After labeling efficiency check, samples were quenched by adding 5% hydroxylamine. The pooled samples were then desalted with Strata × SPE column (Phenomenex) and dried by vacuum centrifugation. (iii) The peptides were separated into 60 fractions by a gradient of 8% to 32% acetonitrile (pH 9.0) for 60 min and then pooled into 4 fractions. IMAC microspheres were used to enrich and collect the phosphopeptides. After washing, the enriched phosphopeptides were eluted with buffer containing 10% NH_4OH. (iv) The elution containing phosphopeptides were collected and lyophilized for LC–MS/MS analysis. The full MS scan resolution was set to 60,000 for a scan range of 350 to 1400 m/z. Up to 25 most abundant precursors were then selected for further MS/MS identification and quantification. (v) The resulting MS/MS data were searched against foxtail millet database v.2.2 (https://phytozome.jgi.doe.gov) using Proteome Discoverer search engine (v.2.4). The fold change value was calculated based on the mean relative abundance value between the compared groups. The phosphosite with fold change more than 1.3 ($P < 0.05$, Student's *t* test) was defined as a differential abundance phosphosite.

RNA-seq analysis and RT-qPCR

WT, *dpy1* mutant (Ci846 background), and transgenic plant *dpy1/Ubipro:SAPK6-3FLAG* were grown under normal conditions for 18 d and then subjected to a 3-d drought treatment. The leaves from 5 plants were pooled as a RNA-seq sample for each of the 3 biological replicates. A total of 18 cDNA libraries were constructed using the NEB Next Ultra II RNA Library Kit (New England Biolabs) and then sequenced with Illumina HiSeq 2500 system (150 bp paired-end reads). For each RNA sample, more than 5.0 Gb of raw data were

generated. The clean reads were aligned to foxtail millet reference genome v.2.2 (https://phytozome.jgi.doe.gov) using HISAT2 (Kim et al. 2015). StringTie (Pertea et al. 2015) was applied to assemble the mapped reads. We compared gene expression profiles of WT, *dpy1*, and *dpy1/Ubipro: SAPK6-3FLAG* plants before and after drought to isolate drought-responsive genes in each genotype and also identified SAPK6-regulated genes by comparison of *dpy1/Ubipro: SAPK6-3FLAG* versus *dpy1* in each condition. Differential expression analysis is processed by DESeq2 (Love et al. 2014) with 3 biological replications. We defined genes with FC > 2 and FDR < 0.05 as DEGs. BR-responsive genes were identified based on our previous RNA-seq data. Briefly, 4,108 DEGs (FC > 2 and FDR < 0.05) were obtained in leaves by comparing transcriptome between BL- and Mock-treated WT plants that were grown under well-watered conditions (Zhao et al. 2020). We then compared these BR-regulated genes with SAPK6-regulated genes under well-watered conditions to investigate BR's possible role in SAPK6 regulation of downstream gene expression.

For RT-qPCR, total RNA was prepared from the leaves treated with 20% PEG6000 solution or drought stress for the indicated times and then digested with DNaseI to remove contaminating DNA. cDNA was synthesized from about 1.5 µg total RNA with RevertAid RT Reverse Transcription Kit (Thermo Scientific). RT-qPCR was performed on the Biorad CFX-96 Real-Time PCR system (Bio-Rad) using the SYBR Green supermix (DBI Bioscience). Foxtail millet ABA biosynthesis genes including *SiNCED1*, *SiNCED4*, *SiABA3*, and *SiAAO3* were the putative orthologs of rice (*O. sativa*), which were obtained by sequence alignment. The expression level of target genes was determined by the comparative threshold cycle method and was normalized to that of foxtail millet *Actin* gene (Seita.7G294000). The primers used for RT-qPCR analysis are listed in Supplemental Data Set S6.

Phylogenetic analysis

The Arabidopsis Genome Initiative, GenBank, and Phytozome were used to obtain the sequence data. The predicted amino acid sequences were aligned by the ClustalW program. The phylogenetic tree was constructed by MEGA5 software with the neighbor-joining method (Saitou and Nei 1987). The source data can be found in Supplemental Files S1 to S6.

Statistical analysis

Student's *t* test and 1-way ANOVA with Tukey's multiple comparisons test were performed with R program (version 4.2.0) (https://www.r-project.org/). Statistically significant differences are indicated by different lowercase letters ($P <$ 0.05, ANOVA) or asterisk (*$P < 0.05$; **$P < 0.01$; ***$P <$ 0.001, Student's *t* test). Summary of statistical analyses can be found in Supplemental Data Set S7.

Accession numbers

Gene accession numbers are available in public databases (https://www.ncbi.nlm.nih.gov/; https://phytozome-next.jgi. doe.gov/) under the following accession numbers: *DPY1* (Seita.5G121100), *SAPK6* (LOC101786757), *SiNCED1* (Seita. 1G288400), *SiNCED4* (Seita.2G035400), *SiABA3* (Seita. 4G266600), *SiAAO3* (Seita.9G061200), *SiBZR1* (Seita.2G3 67800), *SiBRI1* (LOC101765569), and *SiRAF20* (Seita.2G11 7800). The source data of transcriptome and phosphoproteomics have been submitted to a public database, respectively, under the accession codes of PRJEB54684 (EMBL-EBI database, for transcriptome data) and PXD035208 (PRIDE database, for phosphoproteome data).

Author contributions

M.Z. and X.D. designed the research. M.Z., Q.Z., H.L., S.T., W.Z., Y.S., and H.Zhi. performed the experiments. M.Z., S.T., Y.Z., C.Z., H.Zha., G.J., H.W., X.L., D.A., F.Z., and C.W. analyzed the date. M.Z. wrote the paper.

Supplemental data

The following materials are available in the online version of this article.

Supplemental Figure S1. Phylogenetic tree reconstructed from members of the SnRK2 family from Arabidopsis, rice, and foxtail millet.

Supplemental Figure S2. Phylogenetic tree reconstructed from members of B1 to B4 Raf-like MAPKKKs from Arabidopsis, rice, and foxtail millet.

Supplemental Figure S3. The subcellular localization of DPY1 and SAPK6 does not change upon drought stress.

Supplemental Figure S4. *dpy1* is a loss-of-function mutant.

Supplemental Figure S5. Dynamics of soil water contents and soil water potential in the indicated genotypes during drought stress.

Supplemental Figure S6. Repeated drought tolerance phenotypes of the different genotypes in the indicated comparisons.

Supplemental Figure S7. BRZ treatment partially rescues the greater drought sensitivity of *dpy1*.

Supplemental Figure S8. *SAPK6* haplotype variation corresponds with plant drought tolerance in foxtail millet.

Supplemental Figure S9. *SAPK6* overexpression does not rescue the leaf droopiness of *dpy1* plants.

Supplemental Figure S10. Immunoblot detection of SAPK6-3FLAG in randomly selected individuals from the transgenic lines *SAPK6-OE* (*L1*) and *dpy1/SAPK6-OE* (*L8*) using an anti-FLAG antibody.

Supplemental Figure S11. RNA-seq analysis of WT (Ci846), *dpy1*, and *dpy1/SAPK6-OE* plants in response to drought.

Supplemental Figure S12. Quantitative phosphoproteomic analysis and identification of 4 phosphopeptides in endogenous DPY1.

Supplemental Figure S13. Molecular functional annotation of the proteins that are phosphorylated in a DPY1-dependent manner upon osmotic stress.

Supplemental Figure S14. Sequence alignment of the activation loops of SnRK2s in Arabidopsis, rice, and foxtail millet.

Supplemental Figure S15. Osmotic stress–induced SAPK6 phosphorylation is compromised in *dpy1* relative to WT plants.

Supplemental Figure S16. The phosphorylation of SiBRI1 observed in *dpy1* plants strongly decreases to WT levels in response to PEG treatment.

Supplemental Figure S17. MBP can be used as an in vitro substrate for phosphorylation by DPY1.

Supplemental Figure S18. Validation of the induction of DPY1 phosphorylation by drought plus alkaline phosphatase treatment.

Supplemental Figure S19. Identification of 4 phosphopeptides in DPY1-3FLAG IP from *Ubipro:DPY1-3FLAG* transgenic plants treated with PEG or maintained under control conditions.

Supplemental Figure S20. In vitro kinase assays showing that DPY1 cannot directly phosphorylate the kinase-dead variant of SAPK6 (mSAPK6) or SiRAF20 (mSiRAF20).

Supplemental Data Set S1. A full list of DPY1-interacting proteins identified in LC–MS/MS analysis of IP DPY1-FLAG.

Supplemental Data Set S2. Expression changes of DPY1-regulated drought-responsive genes in response to drought among WT, *dpy1*, and *dpy1/SAPK6-OE* plants.

Supplemental Data Set S3. List of SAPK6-activated or repressed genes under drought conditions

Supplemental Data Set S4. List of SAPK6-activated or repressed genes under normal conditions.

Supplemental Data Set S5. List of PEG-induced differential abundance phosphosites in WT and *dpy1* plants.

Supplemental Data Set S6. Primers used in this study.

Supplemental Data Set S7. Summary of statistical analyses.

Supplemental Files S1 to S3. Newick format files of the phylogenetic trees shown in Fig. 2 and Supplemental Figs. S1 and S2.

Supplemental Files S4 to S6. Multiple protein alignments used for the phylogenetic trees shown in Fig. 2 and Supplemental Figs. S1 and S2.

Funding

Conflict of interest statement. None declared.

Data availability

The data that support the findings of this study are available from the corresponding author upon reasonable request.

References

Bang SW, Choi S, Jin X, Jung SE, Choi JW, Seo JS, Kim J-K. Transcriptional activation of rice CINNAMOYL-CoA REDUCTASE 10 by OsNAC5, contributes to drought tolerance by modulating lignin accumulation in roots. Plant Biotechnol J. 2022:**20**(4):736–747. https://doi.org/10.1111/pbi.13752

Belin C, de Franco PO, Bourbousse C, Chaignepain S, Schmitter JM, Vavasseur A, Giraudat J, Barbier-Brygoo H, Thomine S. Identification of features regulating OST1 kinase activity and OST1 function in guard cells. Plant Physiol. 2006:**141**(4):1316–1327. https://doi.org/10.1104/pp.106.079327

Boudsocq M, Barbier-Brygoo H, Laurière C. Identification of nine sucrose nonfermenting 1-related protein kinases 2 activated by hyperosmotic and saline stresses in *Arabidopsis thaliana*. J Biol Chem. 2004:**279**(40):41758–41766. https://doi.org/10.1074/jbc.M405259200

Boudsocq M, Droillard M-J, Barbier-Brygoo H, Laurière C. Different phosphorylation mechanisms are involved in the activation of sucrose non-fermenting 1 related protein kinases 2 by osmotic stresses and abscisic acid. Plant Mol Biol. 2007:**63**(4):491–503. https://doi.org/10.1007/s11103-006-9103-1

Brutnell TP, Wang L, Swartwood K, Goldschmidt A, Jackson D, Zhu X-G, Kellogg E, Van Eck J. *Setaria viridis*: a model for C4 photosynthesis. Plant Cell 2010:**22**(8):2537–2544. https://doi.org/10.1105/tpc.110.075309

Cai Z, Liu J, Wang H, Yang C, Chen Y, Li Y, Pan S, Dong R, Tang G, Barajas-Lopez JDD, et al. GSK3-like kinases positively modulate abscisic acid signaling through phosphorylating subgroup III SnRK2s in *Arabidopsis*. Proc Natl Acad Sci U S A. 2014:**111**(26):9651–9656. https://doi.org/10.1073/pnas.1316717111

Carvalho CM, Santos AA, Pires SR, Rocha CS, Saraiva DI, Machado JPB, Mattos EC, Fietto LG, Fontes EPB. Regulated nuclear trafficking of rpL10A mediated by NIK1 represents a defense strategy of plant cells against virus. PLoS Pathog. 2008:**4**(12):e1000247. https://doi.org/10.1371/journal.ppat.1000247

Chen J, Nolan TM, Ye H, Zhang M, Tong H, Xin P, Chu J, Chu C, Li Z, Yin Y. Arabidopsis WRKY46, WRKY54, and WRKY70 transcription factors are involved in brassinosteroid-regulated plant growth and drought responses. Plant Cell 2017:**29**(6):1425–1439. https://doi.org/10.1105/tpc.17.00364

Chinchilla D, Zipfel C, Robatzek S, Kemmerling B, Nürnberger T, Jones JDG, Felix G, Boller T. A flagellin-induced complex of the receptor FLS2 and BAK1 initiates plant defence. Nature 2007:**448**(7152):497–500. https://doi.org/10.1038/nature05999

Deng J, Kong L, Zhu Y, Pei D, Chen X, Wang Y, Qi J, Song C, Yang S, Gong Z. BAK1 plays contrasting roles in regulating abscisic acid-induced stomatal closure and abscisic acid-inhibited primary root growth in *Arabidopsis*. J Integr Plant Biol. 2022:**64**(6):1264–1280. https://doi.org/10.1111/jipb.13257

Diao X, Schnable J, Bennetzen JL, Li J. Initiation of *Setaria* as a model plant. Front Agric Sci Eng. 2014:**1**(1):16–20. https://doi.org/10.15302/J-FASE-2014011

Fàbregas N, Yoshida T, Fernie AR. Role of Raf-like kinases in SnRK2 activation and osmotic stress response in plants. Nat Commun. 2020:**11**(1):6184. https://doi.org/10.1038/s41467-020-19977-2

Friml J, Gallei M, Gelová Z, Johnson A, Mazur E, Monzer A, Rodriguez L, Roosjen M, Verstraeten I, Živanović BD, et al. ABP1–TMK auxin perception for global phosphorylation and auxin canalization. Nature 2022:**609**(7927):575–581. https://doi.org/10.1038/s41586-022-05187-x

Fu J, Chu J, Sun X, Wang J, Yan C. Simple, rapid, and simultaneous assay of multiple carboxyl containing phytohormones in wounded tomatoes by UPLC-MS/MS using single SPE purification and isotope dilution. Anal Sci. 2012:**28**(11):1081–1087. https://doi.org/10.2116/analsci.28.1081

Gupta A, Rico-Medina A, Caño-Delgado AI. The physiology of plant responses to drought. Science 2020:**368**(6488):266–269. https://doi.org/10.1126/science.aaz7614

Hohmann S. Osmotic stress signaling and osmoadaptation in yeasts. Microbiol Mol Biol Rev. 2002:**66**(2):300–372. https://doi.org/10.1128/MMBR.66.2.300-372.2002

Hua D, Wang C, He J, Liao H, Duan Y, Zhu Z, Guo Y, Chen Z, Gong Z. A plasma membrane receptor kinase, GHR1, mediates abscisic acid- and hydrogen peroxide-regulated stomatal movement in Arabidopsis. Plant Cell 2012:**24**(6):2546–2561. https://doi.org/10.1105/tpc.112.100107

Hu C, Zhu Y, Cui Y, Cheng K, Liang W, Wei Z, Zhu M, Yin H, Zeng L, Xiao Y, et al. A group of receptor kinases are essential for CLAVATA signalling to maintain stem cell homeostasis. Nat Plants. 2018:**4**(4):205–211. https://doi.org/10.1038/s41477-018-0123-z

Jia G, Huang X, Zhi H, Zhao Y, Zhao Q, Li W, Chai Y, Yang L, Liu K, Lu H, et al. A haplotype map of genomic variations and genome-wide association studies of agronomic traits in foxtail millet (Setaria italica). Nat Genet. 2013:**45**(8):957–961. https://doi.org/10.1038/ng.2673

Jia M, Meng X, Song X, Zhang D, Kou L, Zhang J, Jing Y, Liu G, Liu H, Huang X, et al. Chilling-induced phosphorylation of IPA1 by OsSAPK6 activates chilling tolerance responses in rice. Cell Discov. 2022:**8**(1):71. https://doi.org/10.1038/s41421-022-00413-2

Ji J, Yang L, Fang Z, Zhuang M, Zhang Y, Lv H, Liu Y, Li Z. Complementary transcriptome and proteome profiling in cabbage buds of a recessive male sterile mutant provides new insights into male reproductive development. J Proteomics. 2018:**179**:80–91. https://doi.org/10.1016/j.jprot.2018.03.003

Katsuta S, Masuda G, Bak H, Shinozawa A, Kamiyama Y, Umezawa T, Takezawa D, Yotsui I, Taji T, Sakata Y. Arabidopsis Raf-like kinases act as positive regulators of subclass III SnRK2 in osmostress signaling. Plant J. 2020:**103**(2):634–644. https://doi.org/10.1111/tpj.14756

Kim D, Langmead B, Salzberg SL. HISAT: a fast spliced aligner with low memory requirements. Nat Methods. 2015:**12**(4):357–360. https://doi.org/10.1038/nmeth.3317

Kobayashi Y, Yamamoto S, Minami H, Kagaya Y, Hattori T. Differential activation of the rice sucrose nonfermenting1-related protein kinase2 family by hyperosmotic stress and abscisic acid. Plant Cell 2004:**16**(5):1163–1177. https://doi.org/10.1105/tpc.019943

Li B, Ferreira MA, Huang M, Camargos LF, Yu X, Teixeira RM, Carpinetti PA, Mendes GC, Gouveia-Mageste BC, Liu C, et al. The receptor-like kinase NIK1 targets FLS2/BAK1 immune complex and inversely modulates antiviral and antibacterial immunity. Nat Commun. 2019:**10**(1):4996. https://doi.org/10.1038/s41467-019-12847-6

Li J, Wen J, Lease KA, Doke JT, Tax FE, Walker JC. BAK1, an Arabidopsis LRR receptor-like protein kinase, interacts with BRI1 and modulates brassinosteroid signaling. Cell 2002:**110**(2):213–222. https://doi.org/10.1016/S0092-8674(02)00812-7

Lin Z, Li Y, Zhang Z, Liu X, Hsu C-C, Du Y, Sang T, Zhu C, Wang Y, Satheesh V, et al. A RAF-SnRK2 kinase cascade mediates early osmotic stress signaling in higher plants. Nat Commun. 2020:**11**(1):613. https://doi.org/10.1038/s41467-020-14477-9

Liu C, Yu H, Rao X, Li L, Dixon RA. Abscisic acid regulates secondary cell-wall formation and lignin deposition in Arabidopsis thaliana through phosphorylation of NST1. Proc Natl Acad Sci. 2021:**118**(5):e2010911118. https://doi.org/10.1073/pnas.2010911118

Love MI, Huber W, Anders S. Moderated estimation of fold change and dispersion for RNA-seq data with DESeq2. Genome Biol. 2014:**15**(12):550. https://doi.org/10.1186/s13059-014-0550-8

Maeda T, Wurgler-Murphy SM, Saito H. A two-component system that regulates an osmosensing MAP kinase cascade in yeast. Nature 1994:**369**(6477):242–245. https://doi.org/10.1038/369242a0

Mega R, Abe F, Kim J-S, Tsuboi Y, Tanaka K, Kobayashi H, Sakata Y, Hanada K, Tsujimoto H, Kikuchi J, et al. Tuning water-use efficiency and drought tolerance in wheat using abscisic acid receptors. Nat Plants. 2019:**5**(2):153–159. https://doi.org/10.1038/s41477-019-0361-8

Mustilli A-C, Merlot S, Vavasseur A, Fenzi F, Giraudat JRM. Arabidopsis OST1 protein kinase mediates the regulation of stomatal aperture by abscisic acid and acts upstream of reactive oxygen species production. Plant Cell 2002:**14**(12):3089–3099. https://doi.org/10.1105/tpc.007906

Nam KH, Li J. BRI1/BAK1, a receptor kinase pair mediating brassinosteroid signaling. Cell 2002:**110**(2):203–212. https://doi.org/10.1016/S0092-8674(02)00814-0

Nolan TM, Brennan B, Yang M, Chen J, Zhang M, Li Z, Wang X, Bassham DC, Walley J, Yin Y. Selective autophagy of BES1 mediated by DSK2 balances plant growth and survival. Dev Cell. 2017:**41**(1):33–46.e37. https://doi.org/10.1016/j.devcel.2017.03.013

Osakabe Y, Maruyama K, Seki M, Satou M, Shinozaki K, Yamaguchi-Shinozaki K. Leucine-rich repeat receptor-like kinase1 is a key membrane-bound regulator of abscisic acid early signaling in Arabidopsis. Plant Cell 2005:**17**(4):1105–1119. https://doi.org/10.1105/tpc.104.027474

Osakabe Y, Yamaguchi-Shinozaki K, Shinozaki K, Tran LS. Sensing the environment: key roles of membrane-localized kinases in plant perception and response to abiotic stress. J Exp Bot. 2013:**64**(2):445–458. https://doi.org/10.1093/jxb/ers354

Pei D, Hua D, Deng J, Wang Z, Song C, Wang Y, Wang Y, Qi J, Kollist H, Yang S, et al. Phosphorylation of the plasma membrane H+-ATPase AHA2 by BAK1 is required for ABA-induced stomatal closure in Arabidopsis. Plant Cell 2022:**34**(7):2708–2729. https://doi.org/10.1093/plcell/koac106

Pertea M, Pertea GM, Antonescu CM, Chang T-C, Mendell JT, Salzberg SL. Stringtie enables improved reconstruction of a transcriptome from RNA-seq reads. Nat Biotechnol. 2015:**33**(3):290–295. https://doi.org/10.1038/nbt.3122

Saitou N, Nei M. The neighbor-joining method: a new method for reconstructing phylogenetic trees. Mol Biol Evol. 1987:**4**(4):406–425. 10.1093/oxfordjournals.molbev.a040454

Sakata Y, Komatsu K, Takezawa D. ABA as a universal plant hormone. In: **Lüttge U Beyschlag W, Cushman J**, editors. Progress in botany. 75. Berlin: Springer; 2014. p. 57–96.

Santos AA, Carvalho CM, Florentino LH, Ramos HJO, Fontes EPB. Conserved threonine residues within the A-loop of the receptor NIK differentially regulate the kinase function required for antiviral signaling. PLoS One 2009:**4**(6):e5781. https://doi.org/10.1371/journal.pone.0005781

Saruhashi M, Ghosh TK, Arai K, Ishizaki Y, Hagiwara K, Komatsu K, Shiwa Y, Izumikawa K, Yoshikawa H, Umezawa T, et al. Plant Raf-like kinase integrates abscisic acid and hyperosmotic stress signaling upstream of SNF1-related protein kinase2. Proc Natl Acad Sci. 2015:**112**(46):6388–6396. https://doi.org/10.1073/pnas.1511238112

Shang Y, Dai C, Lee MM, Kwak JM, Nam KH. BRI1-associated receptor kinase 1 regulates guard cell ABA signaling mediated by open stomata 1 in Arabidopsis. Mol Plant. 2016:**9**(3):447–460. https://doi.org/10.1016/j.molp.2015.12.014

Shinozawa A, Otake R, Takezawa D, Umezawa T, Komatsu K, Tanaka K, Amagai A, Ishikawa S, Hara Y, Kamisugi Y, et al. SnRK2 protein kinases represent an ancient system in plants for adaptation to a terrestrial environment. Commun Biol. 2019:**2**(1):30. https://doi.org/10.1038/s42003-019-0281-1

Soma F, Mogami J, Yoshida T, Abekura M, Takahashi F, Kidokoro S, Mizoi J, Shinozaki K, Yamaguchi-Shinozaki K. ABA-unresponsive SnRK2 protein kinases regulate mRNA decay under osmotic stress in plants. Nat Plants. 2017:**3**(1):16204. https://doi.org/10.1038/nplants.2016.204

Soma F, Takahashi F, Suzuki T, Shinozaki K, Yamaguchi-Shinozaki K. Plant Raf-like kinases regulate the mRNA population upstream of ABA-unresponsive SnRK2 kinases under drought stress. Nat Commun. 2020:**11**(1):1373. https://doi.org/10.1038/s41467-020-15239-3

Stecker KE, Minkoff BB, Sussman MR. Phosphoproteomic analyses reveal early signaling events in the osmotic stress response. Plant Physiol. 2014:**165**(3):1171–1187. https://doi.org/10.1104/pp.114.238816

Takahashi Y, Zhang J, Hsu PK, Ceciliato PHO, Zhang L, Dubeaux G, Munemasa S, Ge C, Zhao Y, Hauser F, et al. MAP3Kinase-dependent SnRK2-kinase activation is required for abscisic acid signal transduction and rapid osmotic stress response. Nat Commun. 2020:**11**(1):12. https://doi.org/10.1038/s41467-019-13875-y

Tian G, Wang S, Wu J, Wang Y, Wang X, Liu S, Han D, Xia G, Wang M. Allelic variation of TaWD40-4B.1 contributes to drought tolerance by modulating catalase activity in wheat. Nat Commun. 2023:**14**(1):1200. https://doi.org/10.1038/s41467-023-36901-6

Toriyama T, Shinozawa A, Yasumura Y, Saruhashi M, Hiraide M, Ito S, Matsuura H, Kuwata K, Yoshida M, Baba T, et al. Sensor histidine kinases mediate ABA and osmostress signaling in the moss *Physcomitrium patens*. Curr Biol. 2022:**32**(1):164–175 e168. https://doi.org/10.1016/j.cub.2021.10.068

Turner NC. Turgor maintenance by osmotic adjustment: 40 years of progress. J Exp Bot. 2018:**69**(13):3223–3233. https://doi.org/10.1093/jxb/ery181

Umezawa T, Sugiyama N, Mizoguchi M, Hayashi S, Myouga F, Yamaguchi-Shinozaki K, Ishihama Y, Hirayama T, Shinozaki K. Type 2C protein phosphatases directly regulate abscisic acid-activated protein kinases in *Arabidopsis*. Proc Natl Acad Sci. 2009:**106**(41): 17588–17593. https://doi.org/10.1073/pnas.0907095106

Verslues PE, Bailey-Serres J, Brodersen C, Buckley TN, Conti L, Christmann A, Dinneny JR, Grill E, Hayes S, Heckman RW, et al. Burning questions for a warming and changing world: 15 unknowns in plant abiotic stress. Plant Cell 2022:**35**(1):67–108. https://doi.org/10.1093/plcell/koac263

Vlad F, Droillard M-J, Valot B, Khafif M, Rodrigues A, Brault M, Zivy M, Rodriguez PL, Merlot S, Laurière C. Phospho-site mapping, genetic and in planta activation studies reveal key aspects of the different phosphorylation mechanisms involved in activation of SnRK2s. Plant J. 2010:**63**(5):778–790. https://doi.org/10.1111/j.1365-313X.2010.04281.x

Wang X, Li X, Meisenhelder J, Hunter T, Yoshida S, Asami T, Chory J. Autoregulation and homodimerization are involved in the activation of the plant steroid receptor BRI1. Dev Cell. 2005:**8**(6):855–865. https://doi.org/10.1016/j.devcel.2005.05.001

Wang Z-Y, Seto H, Fujioka S, Yoshida S, Chory J. BRI1 is a critical component of a plasma-membrane receptor for plant steroids. Nature 2001:**410**(6826):380–383. https://doi.org/10.1038/35066597

Wang C, Tang S, Zhang Q, Shang Z, Liu X, Diao X, Zhao M. Kinase activity is required for the receptor kinase DROOPY LEAF1 to control leaf droopiness. Plant Signal Behav. 2021:**16**(11):1976561. https://doi.org/10.1080/15592324.2021.1976561

Wu F, Chi Y, Jiang Z, Xu Y, Xie L, Huang F, Wan D, Ni J, Yuan F, Wu X, et al. Hydrogen peroxide sensor HPCA1 is an LRR receptor kinase in *Arabidopsis*. Nature 2020:**578**(7796):577–581. https://doi.org/10.1038/s41586-020-2032-3

Yang C, Shen W, He Y, Tian Z, Li J. OVATE family protein 8 positively mediates brassinosteroid signaling through interacting with the GSK3-like kinase in rice. PLoS Genet. 2016:**12**(6):e1006118. https://doi.org/10.1371/journal.pgen.1006118

Zhang B, Wang X, Zhao Z, Wang R, Huang X, Zhu Y, Yuan L, Wang Y, Xu X, Burlingame AL, et al. OsBRI1 activates BR signaling by preventing binding between the TPR and kinase domains of OsBSK3 via phosphorylation. Plant Physiol. 2016:**170**(2):1149–1161. https://doi.org/10.1104/pp.15.01668

Zhao Z, Tang S, Li W, Yang X, Wang R, Diao X, Tang W. Overexpression of a BRASSINAZOLE RESISTANT 1 homolog attenuates drought tolerance by suppressing the expression of PLETHORA-LIKE 1 in *Setaria italica*. Crop J. 2021:**9**(5):1208–1213. https://doi.org/10.1016/j.cj.2021.02.006

Zhao M, Tang S, Zhang H, He M, Liu J, Zhi H, Sui Y, Liu X, Jia G, Zhao Z, et al. DROOPY LEAF1 controls leaf architecture by orchestrating early brassinosteroid signaling. Proc Natl Acad Sci. 2020:**117**(35): 21766–21774. https://doi.org/10.1073/pnas.2002278117

Zhu J-K. Abiotic stress signaling and responses in plants. Cell 2016:**167**(2):313–324. https://doi.org/10.1016/j.cell.2016.08.029